APPLIED PHYSICS REVIEWS—FOCUSED REVIEW

Plasma physics of liquids—A focused review

Patrick Vanraes and Annemie Bogaerts
PLASMANT, Department of Chemistry, University of Antwerp, Universiteitsplein 1, 2610 Wilrijk-Antwerp, Belgium

(Received 22 December 2017; accepted 23 May 2018; published online 25 July 2018)

The interaction of plasma with liquids has led to various established industrial implementations as well as promising applications, including high-voltage switching, chemical analysis, nanomaterial synthesis, and plasma medicine. Along with these numerous accomplishments, the physics of plasma in liquid or in contact with a liquid surface has emerged as a bipartite research field, for which we introduce here the term "plasma physics of liquids." Despite the intensive research investments during the recent decennia, this field is plagued by some controversies and gaps in knowledge, which might restrict further progress. The main difficulties in understanding revolve around the basic mechanisms of plasma initiation in the liquid phase and the electrical interactions at a plasma-liquid interface, which require an interdisciplinary approach. This review aims to provide the wide applied physics community with a general overview of the field, as well as the opportunities for interdisciplinary research on topics, such as nanobubbles and the floating water bridge, and involving the research domains of amorphous semiconductors, solid state physics, thermodynamics, material science, analytical chemistry, electrochemistry, and molecular dynamics simulations. In addition, we provoke awareness of experts in the field on yet underappreciated question marks. Accordingly, a strategy for future experimental and simulation work is proposed. *Published by AIP Publishing*. https://doi.org/10.1063/1.5020511

TABLE OF CONTENTS

I. INTRODUCTION 1
II. PLASMA INITIATION IN LIQUIDS: ELECTRICAL PROPERTIES OF THE BULK LIQUID 3
A. A polarized debate on plasma initiation 3
B. Electronic mechanism: Are liquids sloppy solids in disguise? 5
C. Bubble mechanism: The existential crisis of nanobubbles 11
D. Interface mechanism: Through the eye of the needle electrode 13
E. Liquids in strong fields: Can the floating water bridge help us cross the knowledge gap? 16
III. PLASMA-LIQUID INTERACTION: ELECTRICAL PROPERTIES OF THE LIQUID SURFACE 17
A. Electrical coupling of the worlds above and beneath: A not-so-superficial surface 17
B. Surface ion release: Surfing on capillary waves and Taylor cones 19
C. Surface electron release: To be or not to be solvated, that is the question 21
D. Electrical properties of surface vapor: Into the mysteries of the mist 23
IV. THE FUTURE OF PLASMA PHYSICS OF LIQUIDS 25

I. INTRODUCTION

Over 99% of the observable universe is made of plasma. About 71% of the planet we live on is covered by liquid. Yet, the interaction between both states of matter does not occur so often in nature on Earth and for that reason it is described by a specialized and rather young research domain. The importance of this part of plasma physics is undeniably illustrated with the various established and promising applications of plasma-liquid systems. Current industrial implementation can be found in high-voltage switching,[1] electrical discharge machining,[2] chemical analysis,[3,4] and food processing.[5] Next to that, the versatility of this technology has recently led to the development of numerous reactor types that are proposed for water treatment,[6–8] shockwave production,[9] polymer solution treatment,[10] chemical synthesis of H_2 and H_2O_2,[11,12] nanomaterial synthesis,[13,14] and extraction of biocompounds.[15] Furthermore, biological material is naturally surrounded by a liquid layer, and thus its interaction with plasma also belongs to this field. Observations that plasma treatment induces faster germination and more effective growth of plants are responsible for the emerging field of plasma agriculture.[16] Similarly, the successful use of plasma for wound healing, skin treatment, dentistry, and cancer treatment has provoked a rapidly growing interest in

plasma medicine in recent years.[17–19] Most of these proposed applications have emerged after the start of the new millennium, amplifying a new wave of interest in the field.

Despite this recent progress, a fundamental understanding of the underlying processes in these applications is still missing, due to different impediments. A first complexity is caused by the wide variety in plasma-liquid reactors. Classification methods can be based on plasma regime, i.e., corona, glow, arc, or dielectric barrier discharge, on the applied voltage waveform, i.e., DC, AC (low frequency), radio frequency, microwave or pulsed discharge, or on the plasma-liquid phase distribution and electrode configuration. Considering the latter approach, Vanraes *et al.* identified 107 different plasma reactor types in a literature study of around 300 scientific reports on the application of water treatment.[20] Categorization of these reactors resulted in the identification of six main classes, viz., in-liquid discharge, gas phase discharge over a liquid surface, bubble discharge, spray discharge, remote discharge, and hybrid reactors (Fig. 1). To make things even more complicated, an extension of this classification is possible, including, for instance, surface discharge on a gas-liquid,[21–28] liquid-liquid,[29] or liquid-solid[30–34] interface. Although a few attempts have been made to compare distinct types of plasma-liquid systems, especially in the context of water treatment (see, e.g., Refs. 35–38), one should keep in mind that the underlying fundamental processes strongly depend on the specific reactor configuration, materials, and operating conditions.

As a second complexity in this subfield of plasma physics, the application of several plasma diagnostic methods is hindered by the surrounding liquid and the often complicated discharge geometry. Additional difficulties arise as the liquid properties change in time under influence of plasma interaction, thus hampering the reproducibility of successive experiments. Moreover, such experiments generally suffer from an unsteady electrode shape, for in-liquid discharge due to erosion of the submerged electrodes, and for gas phase discharge due to sputtering, evaporation, and oscillation of the liquid electrode surface. Since the plasma behavior generally is very sensitive to these experimental conditions, a small deviation in them can lead to a tremendous divergence in the observed results, resulting in seemingly contradicting studies. This is the corner stone of the barrier that stands between scientists in this domain and the definite answers they seek.

In the 2012 Plasma Roadmap,[39] two key challenges were formulated for this field: (1) determining the initiation and propagation mechanisms of in-liquid discharge and (2) identifying the fundamental physical and chemical processes at the plasma-liquid interface. As clearly stated in the more recent 2016 Roadmap on plasma-liquid interactions[40] and the 2017 Plasma Roadmap,[41] these challenges still remain today. Concerning the first challenge, several recent reviews have discussed the possible underlying mechanisms of voltage-induced breakdown in liquids.[42–54] Next to that, a few reviews have addressed the second challenge as well.[40,55–57] These reviews are very informative and inspiring, but we believe that the field would benefit from more interaction with closely related research areas, such as laser-induced breakdown in liquids, electrical breakdown of solids, plasma-solid interaction, analytical chemistry, electrochemistry, nanobubbles, the floating water bridge, thermodynamics, hydrodynamics, and molecular dynamics simulations of the solvated electron. Scientists active on these research topics are generally not familiar with the above-mentioned challenges in the plasma physics of liquids that they can collaborate on, while fundamental insights from these neighboring domains can prove to be key issues towards finding resolution. Therefore, it is crucial to open the borders around this research domain in both directions.

Accordingly, the aim of this focused review is twofold. First, we want to motivate the wide applied physics

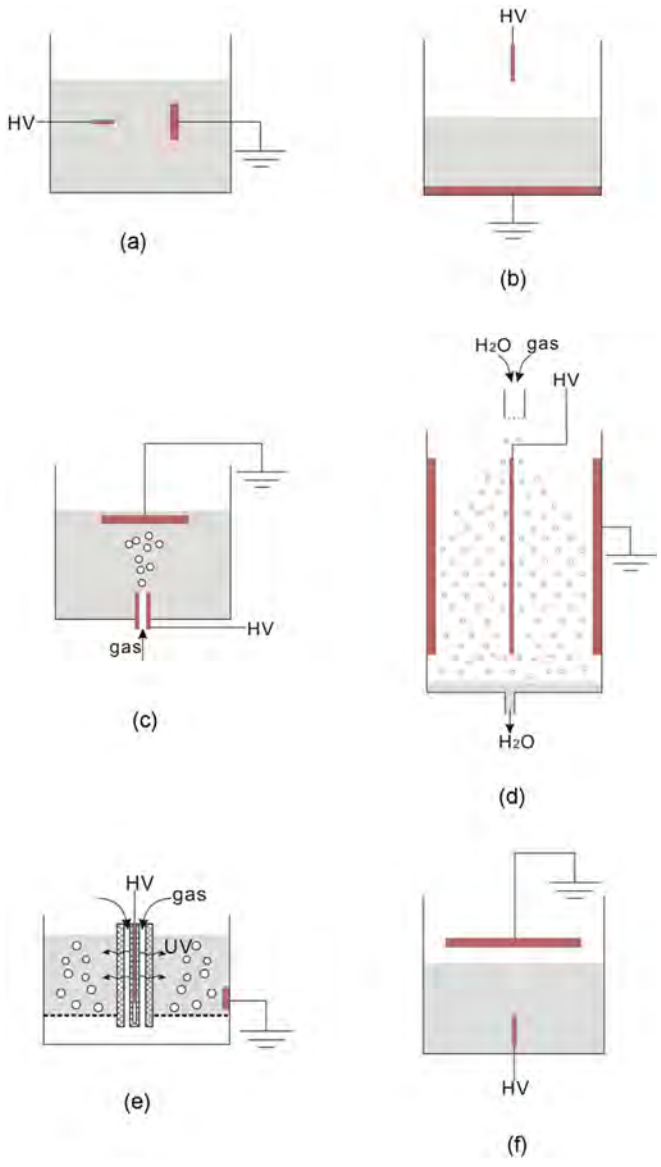

FIG. 1. The six main plasma-liquid reactor types, according to Ref. 20: (a) in-liquid discharge (here represented with the commonly used pin-to-plate configuration), (b) gas phase discharge over a liquid surface, (c) bubble discharge, (d) spray discharge, (e) remote discharge, where plasma is generated not in direct contact with the liquid, and (f) hybrid reactors, which combine any of the other types (e.g., in-liquid and gas phase discharge in this scheme). HV stands for high voltage and UV for ultraviolet radiation. The liquid phase is represented in grey, the electrodes in red, and dielectric barriers [in (e)] with cross hatching. From P. Vanraes *et al.*, *Plasma Science and Technology: Progress in Physical States and Chemical Reactions. Copyright 2016* InTech. Reprinted with permission from InTech.

community to collaborate in interdisciplinary research required to address the mentioned research challenges. Second, we want to propose possible answers to some of the prominent fundamental question marks in the physics of plasma in or in contact with liquids, based on recent insights from various related fields. For this purpose, we provide a concise overview of the state-of-the-art to non-experts, while presenting alternative perspectives to experts. Specifically, this review focusses on the fundamental mechanism of plasma initiation in liquid and the electrical processes involved in plasma-liquid interaction. For this reason, we will mainly consider in-liquid discharges [Fig. 1(a)] in Sec. II and gas phase discharge in contact with liquids [Fig. 1(b)] in Sec. III, as they represent the two general cases that are referred to in the above-mentioned key challenges. We will pay particular attention to water, for which we identified some particular controversies on the fundamental mechanisms.

Considering that the title of this review, "plasma physics of liquids," is currently not yet commonly used in the scientific community, it first requires some clarification. First and foremost, we believe the term is concise and effective, in the way that it immediately can be understood as the part of plasma physics that deals with liquids. Second, the term deliberately invokes the question whether liquids can be plasmas. Consider, for instance, a thought experiment where a body of liquid is first evaporated, then transformed into a plasma state and subsequently shrunk down to the size of a liquid again. Will the result be plasma, liquid, or maybe both? This question is of particular interest in the context of plasma initiation in the liquid phase. In this light, the term "plasma physics of liquids" is inherently associated with plasma generation in liquids, while it is broad enough to comprise the topic of plasma in contact with liquids as well. Therefore, we believe it to be a suitable term to address the bipartite subfield of plasma physics that deals with both in-liquid plasma and plasma-liquid interaction and we intend to introduce it as such.

The bipartite nature of plasma physics of liquids as a research domain is adopted in the structure of the review. The first half of the review (Sec. II) focusses on the fundamental mechanisms of plasma initiation in liquids. After explaining the existing debate on this issue, we explore the controversial idea to describe the electrical behavior of liquids with models originally constructed for solids. Next, the role of the naturally present nanobubbles in the liquid and of the oxide layer on the electrode is discussed. To conclude the first half, we suggest seeking deeper insight in the study of liquids in strong electric fields without plasma formation, using the example of the floating water bridge. In the second half of the review (Sec. III), the focus is shifted towards the electrical properties of a liquid surface in contact with plasma. First, the interdependence of the plasma behavior and processes in the liquid is demonstrated. Next, we consider the mechanisms of ion emission from the surface, based on literature on ambient desorption ionization. In order to illuminate electron emission from a liquid electrode (pun intended), we once again address the above hypothesis to model liquids as solids. Afterwards, the influence of vapor, clustering and micro- or nanosized droplets at the liquid surface is examined. Section IV finally summarizes the main achievements in the field and suggests future steps to encourage faster progress.

II. PLASMA INITIATION IN LIQUIDS: ELECTRICAL PROPERTIES OF THE BULK LIQUID

A. A polarized debate on plasma initiation

The research history of plasma formation in the liquid phase goes back to the second quarter of the previous century,[58] when investigations were mainly stimulated by the application of insulating transformer oil. Already at this early stage, two opposing plasma initiating mechanisms were postulated for voltage-induced breakdown at a submerged electrode. One school of thought, indicated as the *electronic mechanism*, suggested electrical discharge to be generated purely by electric processes in the liquid phase.[58] According to the rivaling *bubble mechanism*, plasma initiation occurs in a gas phase, i.e., a bubble.[58] As such, everything boiled down to a fundamental dilemma—which comes first: plasma or bubble? In other words, does ionization precede evaporation or vice versa? The available evidence at that time, however, could only indirectly speak in favor of one or the other mechanism, due to the limitations of experimental techniques and materials. More accurate time-resolved measurements and high voltage pulses into the nanosecond time scale and below were made possible during the eight decennia that followed, due to major advancements in diagnostic methods and pulsed power technology.[40] With this progress, the door seems opened towards a clear-cut answer. Yet, the very same debate between plasma physicists continues to this day, as both postulated mechanisms survived the tooth of time.[40]

When faced with such a chicken-or-egg problem, it is essential to clearly define the chicken and egg. What do plasma physicists, for instance, mean with a bubble? The answer to this question is at least twofold. Specialized literature refers to either a pre-existing microbubble or the formation of a low density region in the liquid. Several bubble formation mechanisms have been proposed, such as local Joule heating in the liquid,[46,59] electrochemical effects,[46] electrostatic expansion of existing bubbles,[57] and electrostriction.[60] As these mechanisms obviously involve electrical processes, how is the chicken, the electronic mechanism, exactly defined? Basically, it encapsulates all ionization mechanisms that occur directly in the liquid phase. Examples include electron-induced processes, such as electron multiplication by direct impact ionization and the Auger effect, as well as field-induced phenomena, involving field ionization or field dissociation of liquid or solvated molecules.[51] Also, the role of photoionization mechanisms originating from background or produced radiation cannot *a priori* be excluded.

The electronic mechanism has mainly received criticism based on theoretical counter-arguments. For example, many researchers considered electron multiplication in the liquid phase unlikely due to the strong scattering effects that are expected for such high density. Yet, electron avalanches have already been observed in liquid argon,[61–63] xenon,[64–66] nitrogen,[61] sulfur,[67] cyclohexane,[68,69] and propane.[69] For

cryogenic liquids, the lower breakdown strength of the liquid phase as compared to the gaseous phase has been explained with the absence of inelastic electron energy losses in liquid.[70,71] In recent years, electron multiplication in liquid noble gases has even found promising application in cryogenic avalanche detectors for medical diagnostic techniques, including positron emission tomography, and rare-event experiments, such as direct dark matter search, astrophysical neutrino detection, and coherent neutrino-nucleus scattering (see Refs. 72 and 73 for two reviews). Interestingly, cryogenic hole avalanches form the fundamental mechanism in alternative so-called "liquid-hole multipliers."[74,75] For the case of water, a recent study suggests electron multiplication in the liquid phase to be possible with a high local electric field of 3.0×10^9 V/m at a submerged sharp high voltage pin electrode, based on experiments and modeling.[59] The corresponding model made use of the so-called *dense gas approximation*, where concepts are taken from gas discharge physics in order to model the liquid as a highly compressed gas. The electronic mechanism for water also found support in Ref. 76, based on the measurement of an initial pressure of 5.8 GPa at the sharp electrode tip.

For the bubble mechanism, on the other hand, phase change prior to plasma initiation can currently only be explained for voltage pulse durations of the order of 10 μs or higher,[49] while plasma in pre-existing microbubbles is initiated in the order of microseconds.[77] For sub-nanosecond pulses resulting in an inhomogeneous field, an electrostriction mechanism has recently been proposed,[60] according to which nano-sized pores are formed due to deformation and discontinuities in the liquid at high local electric fields.[78] This electrostriction model is in agreement with the observed changes in the liquid density and refractive index in the vicinity of a high voltage pin electrode, as observed by means of fast Schlieren imaging.[79–81] However, a change in refractive index has similarly been observed in Ref. 82 with a local electric field around 10^7 V/m, below the plasma initiation threshold of water, where it was attributed, in contrast, to the measured excitation of OH stretch vibration in water molecules. Comparable observations were reported in Ref. 83 for fields up to 4×10^8 V/m, still below the threshold. The authors of the latter study explained the refractive index change with dipole reorientation of the water molecules and suggested a reorientation saturation around 3×10^8 V/m.

Hence, after decennia of brooding over this chicken-or-egg problem, no universal answer hatched out. Instead, experiments seem to suggest that both chicken and egg can be valid answers, depending on the circumstances. As already explained in the introduction, a small deviation in experimental settings can result in dissimilar observations. Accordingly, there is a growing agreement between plasma scientists that the applied voltage pulse rise time and duration are crucial factors for the initiating mechanisms.[40,51,54,84] The difference in electrical properties between polar liquids, such as water, and nonpolar liquids, like transformer oil, are also regularly emphasized.[40,47,48,54] One should, however, consider the role of many other parameters as well, including liquid viscosity, heat capacity, conductivity, temperature and gradients thereof, chemical processes, impurities and electrode shape, material and surface conditions. From the variety and complexity of these influences, it is clear that research efforts will need to go through fire and water to link the experimental observations with the underlying physics, in order to get to the bottom of plasma formation in liquids.

The scientific challenges on voltage-induced plasma formation in the liquid phase do not end here, as the succeeding discharge evolution is insufficiently understood as well. In contrast to the hidden initiation mechanisms, the further plasma evolution is nevertheless more easily accessible by means of time- and space-resolved imaging and spectroscopic diagnostics. Correspondingly, a great deal of experimental data on this topic can be found in literature (see, e.g., Refs. 47, 48, 51, and 85). Here, we will only give a short overview. After the plasma initiation process, one or more conductive channels are formed at the electrode tip. In Fig. 2, for instance, several channels emerge between t = 4 and 5 ns. Each channel, answering to the name *streamer*, has a width of about 10 μm and is believed to consist of gaseous plasma.[86–89] It has a spherical head characterized by a strong local electric field, which propagates away from the electrode with a velocity ranging from 100 m s^{-1} to 100 km s^{-1}.[48,51] The plasma gas inside the streamer, which is near local thermodynamic equilibrium, mainly originates from liquid molecules, while the contribution of dissolved gases is marginal.[40] The gas temperature ranges up to 5000 K and its ionization degree can exceed 10%.[57] Streamers often have a tree-like structure with several branches, as clearly visible in Fig. 2. Branching of a propagating streamer has been explained as an interaction of the streamer head with inhomogeneities and microbubbles.[90,91] Depending on the experimental conditions, such as voltage amplitude and polarity, interelectrode distance and liquid type, at least four modes of streamers are observed, with differences in velocity, structure and behavior,[48,53,85] i.e., a first, second, third and fourth mode, according to the order of magnitude of their velocity, 10^2, 10^3, 10^4, and 10^5 m s^{-1}, respectively.[48] Accordingly, different mechanisms are proposed for these modes. The *supersonic mechanism* applies to fast streamers ($\sim 10^3$ to 10^5 m s^{-1}), as it involves ionization processes in the liquid phase, in clear analogy with the electronic mechanism.[85,92] The *subsonic mechanism*, on the other hand, concerns the stepwise propagation of slow streamers ($\sim 10^2$ m s^{-1}) induced by electron avalanches in successive vapor bubbles, similar to the bubble mechanism.[57,85,92]

For more detailed information on the above-mentioned initiation and propagation mechanisms of electrical discharge in liquids, we refer to the reviews in Refs. 48, 51, 54, and 85. In addition, two other recent reviews are centered around the bubble mechanism in the case of pre-existing bubbles.[42,44] In what follows, we will zoom in on important aspects that were left out of focus in the debate up to now.

Figure 3 presents an overview of the main topics of Sec. II and their interconnections. Sections II B and II C will deal with topics related to the electronic mechanism and the bubble mechanism, respectively. In Sec. II D, we will postulate a third class of plasma initiation mechanisms in liquids, termed the *interface mechanism*, where electrical discharge

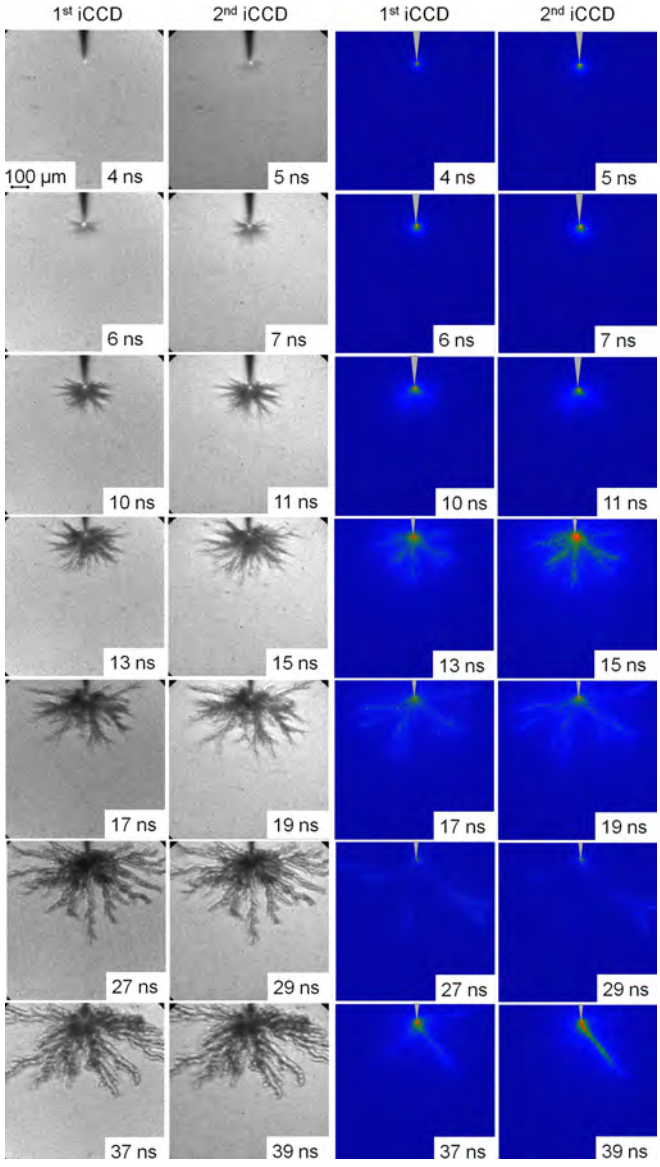

FIG. 2. Plasma initiation and branched streamer progression in deionized water under a 15 kV positive pulse, measured using two synchronized iCCD cameras, by means of shadowgraph photography to visualize the streamers (left) and light emission imaging, showing where plasma is most intense (right). Reproduced with permission from I. Marinov *et al.*, J. Phys. D: Appl. Phys. **47**(22), 224017 (2014). Copyright 2014 IOP Publishing.

inception processes occur in the electrode surface layer, based on breakdown mechanisms in solids. Finally in Sec. II E, we will investigate the current knowledge on liquid properties in the presence of a strong electric field without plasma formation by means of the floating liquid bridge, in order to gain a better understanding of the plasma initiation mechanisms. As should be noted, the study of electrical processes at the plasma-liquid interface in Sec. III is also applicable to the surface of propagating streamers in liquid or to the bubble surface in the bubble mechanism.

B. Electronic mechanism: Are liquids sloppy solids in disguise?

Plasma physicists tend to approach the liquid phase as if it were a dense gas. The extensive use of the term "fluid" in the field illustrates this trend. Besides that, such attitude can be noticed, for instance, throughout the thermodynamic description of plasma liquids and – to a certain extent – liquid plasmas (see, e.g., Refs. 93 and 94) This also reminds to the gaseous plasma model of the Sun, which has been dominantly used for several past decennia and which soon might be decrowned by the rivaling new liquid model.[95] Other striking examples are the recently developed 0D chemical kinetics models for aqueous chemistry under plasma treatment, which are very similar to the models used for plasma gases.[96–99] Next to that, a dense gas approximation has occasionally been applied to estimate electric field threshold values for plasma initiation in liquids.[54,59,100] As such, criticisms to the electronic mechanism are often formulated from this perspective as well. As already mentioned in Sec. II A, many plasma physicists are still reluctant to accept the electronic mechanism due to the dominant electron scattering processes they presume at such high density.[44,46,51,57] If the high liquid density were the only base of this argument, it would have been easily contradicted. That is, solid metals and semiconductors have similar density, yet display a high electron mobility. The criticism therefore has a second, more implicit foundation: liquids, as condensed interacting gases, cannot be readily compared with solids. Their structure is amorphous and continuously changes in time. As such, liquids are assumed to behave dissimilar to solids in various ways (see, e.g., Refs. 46, 51, and 57).

We hereby challenge this idea. Although it is intuitively appealing to think of liquids as dense gases, some indications can be found in literature that comparison with solids regarding their electronic, optical and thermodynamic properties is generally more suitable.[101–103] As a first example, liquid metals display similar electronic behavior to their solid counterparts, despite their amorphous and changing ion structure.[102] They possess an electron cloud as well, although it is modified in comparison to solid metals and electrons sometimes get trapped in interstitial voids of the liquid.[102] The theory on their structure and electronic properties is still at a primitive stage, since complex quantum dynamic effects play a dominant role.[104–106] Metal-insulator transitions in liquid metals can occur under different circumstances and are a topic of intensive research.[104,105,107,108] *Ab initio* quantum molecular dynamics simulation based on density functional theory provides nowadays the best tool to assess these properties.[104,105]

Second, dielectric liquids seem to behave electrically the same as amorphous semiconductors on short time scales. Electronic and photonic processes namely have the characteristic feature to occur during small time intervals, in which molecular diffusion is not important. The liquid therefore appears frozen in time from the perspective of photons and electrons. Accordingly, an amorphous semiconductor model is increasingly applied by experts to explain pulsed laser-induced breakdown in dielectric liquids with pulse durations in the order of nanoseconds or below.[103,109–111] Water, for instance, has often been modeled with a band gap of 6.5 eV,[112] although recent studies propose to apply a higher value of 8 eV,[113] 8.7 to 8.9 eV,[114,115] or 9.5 eV.[103] Initially, the liquid molecules get ionized via multiphoton absorption

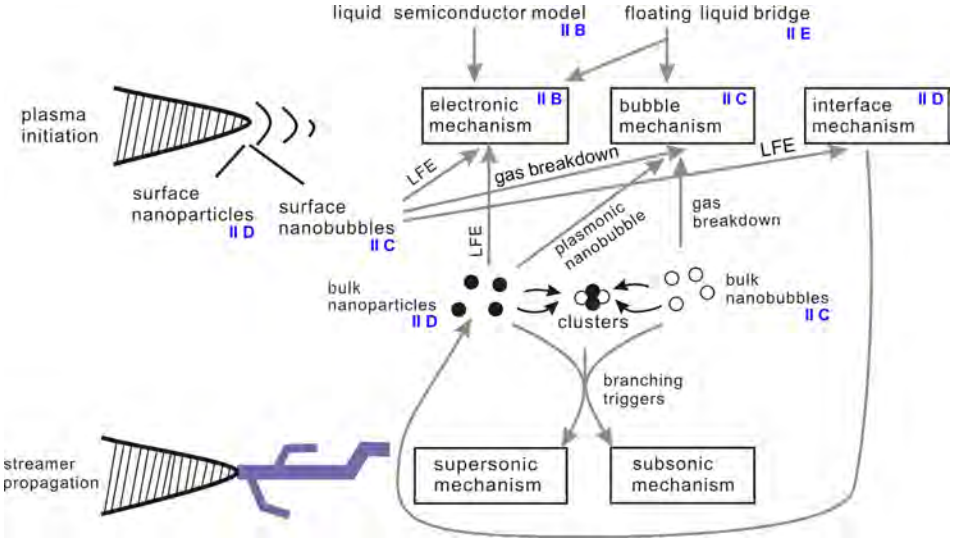

FIG. 3. Schematic overview of Sec. II, showing the interdependence of the central topics. The blue codes refer to the corresponding subsection numbering. LFE stands for local electric field enhancement.

as well as tunneling,[111] bringing the released electrons in the conduction band of the liquid. Next, the conduction band electrons are accelerated by the optical field via inverse Bremsstrahlung until they acquire sufficient kinetic energy for dissociative attachment collisions with H_2O[111] or for H_2O ionization by direct impact. Finally, a phase transition into gaseous plasma takes place, associated with a shock-wave.[116] Electron densities from 10^{17} to $10^{20}\,cm^{-3}$ have been measured during laser-induced breakdown in water.[117,118]

Third, the optical similarities between solids and liquids are well-known.[119] As mentioned above, photons experience liquid media as frozen in time and therefore they cannot distinguish them from solid media. Refraction is observed in both transparent solids and liquids, with refractive indices ranging mostly beyond 1.3, whereas gases are more similar to vacuum in this respect. Also dispersion effects are interchangeable between the two condensed states of matter. Next to that, both phases can display internal and external reflection. Again, these phenomena are generally absent for gases.

Fourth, liquids have more thermodynamic aspects in common with solids than with gases. The density of liquids and solids is nearly identical, making it possible to generate similar shear waves in both, unlike in gases.[120] Liquid can, however, not support all the shear waves as a solid does. Low frequencies are not sustained in liquids, as a corresponding shear wave would dissolve quickly into the liquid fluidity.[121] Shear waves occur above the threshold frequency τ^{-1}, with τ defined as the liquid relaxation time, i.e., the average time between two successive atomic jumps at one location in space.[120,122] This frequency serves as a key parameter of a liquid, responsible for most of its thermodynamic properties.[121] Correspondingly, the phonon theory of solid thermodynamics has recently been translated into a congruent theory for liquids that covered both classical and quantum regimes.[101] The heat capacity of 21 liquids as calculated with this novel phonon theory was found to be in good agreement with experimental values. As a result, liquid energy and specific heat are essentially vibrational, as they are in a solid, while liquid entropy exceeds solid entropy according to the expectations.[123] This conclusion only holds for sufficiently low temperature, where $\tau > 10\tau_D$, with τ_D the Debye vibration period.

We do not want to advocate a view here where liquids are seen as generally more comparable to solids than to gases. In many aspects of their fluidity, liquids and gases have commonalities as well. Neither do we recommend classifying liquids in their overall behavior as an intermediate state between solids and gases. Despite the striking resemblances at both sides, liquids remain unique systems in their own class with a notably mixed dynamical state, in line with the insights of Ref. 124. Instead, we want to motivate physicists in research on liquids to seek inspiration beyond the limiting scope of their studies, not only in the knowledge on the gaseous state of matter, but also on solids. That is, science aims essentially at finding structure in nature. While this movement is lately noticed in the study of laser-induced breakdown of liquids,[103,109,111] the parallels between liquids and solids seem vastly ignored for voltage-induced breakdown up to now.

Considering the noticeable resemblances between solids and liquids in their electronic, photonic and phononic behavior for short times, their plasma breakdown mechanisms are expected to display similarities as well. Note that this expectation only counts for fast processes, including the electronic and supersonic mechanism. Additionally, it is advised to seek similarities mostly between congruent types of liquids and solids. For instance, polymeric liquids should be set side by side with polymeric solids, while polar or nonpolar liquids with small molecular solvent size are better compared with polar or nonpolar amorphous semiconductors. Keeping that in mind, what can we learn from the knowledge on breakdown phenomena in solids?

In insulating solid polymers for high voltage technology, many precursors to electric breakdown have been identified. Directly related to the material structure, important breakdown precursors are gas trapping, micrometer- and submicrometer-sized voids and impurities.[125] Interestingly, metallic inclusions turn out to be less dangerous in this

respect than mineral impurities.[126] Further, unidirectional mechanical stress can induce additional defects in the structure, which can be relevant to the liquid polymer case in the presence of shockwaves or external pressure. Solid polymers under electrical stress exhibit the release of included gas, resulting in their outgassing,[125] which is therefore also expected for polymeric liquids. The electronic structure of polymers can be understood with a band gap model. The band structure formation of polyethylene, for instance, from the orbital levels of the parent alkane series (C_nH_{2n+2}) is illustrated in Fig. 4(a). For growing molecular size, the orbital number increases, leading to a smaller separation between the orbital electrons, up to the point where they can be considered as continuous bands. In a realistic situation, different defects in the amorphous structure of the polymer need to be taken into account, originating in deep and shallow trapping levels, as explained in the caption of Fig. 4(b). For detailed information on several atomistic and macroscopic models for charge transport and breakdown of solid polymers, we refer to the review in Ref.127. Remarkably, the authors of the latter review mention that macroscopic models are developed more from a system- than from a material-oriented research perspective, making them applicable to liquids as well. Hence, we build further on this idea in that the atomistic models can serve as additional inspiration. More recent insights can be taken from the work of Sun *et al*., which is built on *ab initio* molecular dynamics simulation.[128–130]

In amorphous semiconductors, electron multiplication by impact ionization has a long history of research due to its high potential for applications in high voltage switching diodes, see, e.g., Refs. 132–135. Recent interest is driven by the implementation of these semiconductors in X-ray imaging devices and harpicon tubes.[136] In contrast to most solid insulators, the electron avalanche breakdown mechanism—if it can be called this way—is reversible, as in gases and liquids. Amorphous selenium is the most studied example with electron multiplication starting at electric fields from 8×10^7 V/m,[134,135] while other amorphous semiconductors display a higher breakdown threshold. Although this electronic switching behavior is still not fully understood, it has been successfully described with different models. The percolation model uses a phenomenological approach, based on the concept of field-assisted ionization of traps.[137] It considers the interaction of isolated conductive clusters in the amorphous material as a manifestation of its switching behavior, which leads to the redistribution of local electric fields and electron emission probabilities in non-conductive regions. When a conductive cluster connects both electrodes, the breakthrough current appears, followed by the formation of a current filament through Joule heating. The model is supported by experimental data on chalcogenide semiconductor glasses. The so-called lucky-drift model is a semiclassical approach originally proposed by Ridley to explain electron avalanches in crystalline semiconductors.[138] This model has been extended by Rubel *et al*. with the inclusion of elastic charge carrier scattering on the disorder potential inherent to amorphous materials.[139] As shown in Fig. 5, a conducting charge carrier (h^+) with zero initial kinetic energy is accelerated in a direction described by the electric field. During its trajectory, it is scattered elastically by a disorder potential and acoustic phonons and inelastically via optical phonon emission, until impact ionization takes place. The extended model provided a good estimation of the electric field threshold value for breakdown in amorphous selenium and resolved the long-standing question on the lack of electron avalanches in hydrogenated amorphous silicon by revealing its high threshold field.[136] Later, the model was further optimized by Rubel *et al*. to give even more accurate values for the threshold field.[140]

Whereas the lucky-drift model in its current form does not explicitly distinguish between polar and nonpolar semiconductors, this difference needs to be kept in mind. The importance of the semiconductor polarity is most easily understood in terms of the polaron, as introduced by Landau and Pekar.[141] The polaron is a quasi-particle associated with the deformation of an atomic or molecular lattice under influence of a charge carrier, due to Coulomb interaction. As the charge carrier travels through the lattice, it is followed by the deformation, which is therefore sometimes referred to as

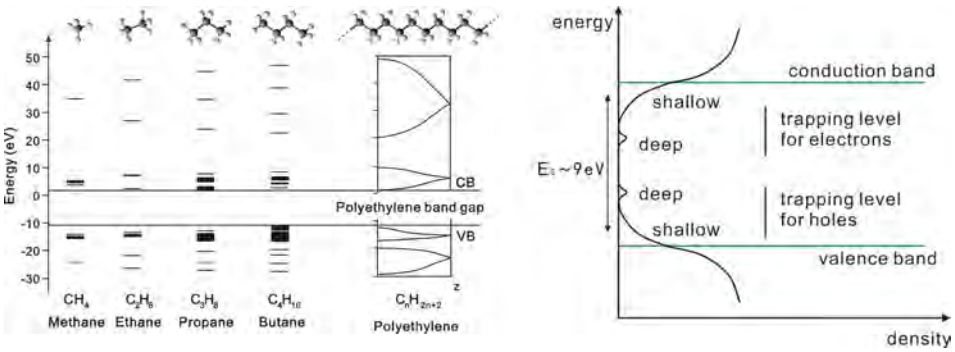

FIG. 4. (Left) Distribution of orbital levels going from methane to polyethylene, according to the ideal case, with the formation of a conduction band (CB) and a valence band (VB). (Right) Realistic band gap model of a general amorphous polymer, taking into account modifications to the ideal band gap scheme. Localized shallow trapping states for electrons are introduced at the border of the forbidden gap by "physical" nonuniformity originating from the different possible conformations of the same polymer molecule. Deep electron traps, on the other hand, find their origin in "chemical" disorder, related to side chains, additives and impurities in the polymer. Figure (a) is adapted with permission from R. Hoffmann *et al*., Macromolecules **24**(13), 3725–3746 (1991).[131] Copyright 1991 American Chemical Society. Figure (b) is reprinted with permission from G. Teyssedre and C. Laurent, IEEE Trans. Dielectr. Electr. Insul. **12**(5), 857–875 (2005). Copyright 2005 IEEE.

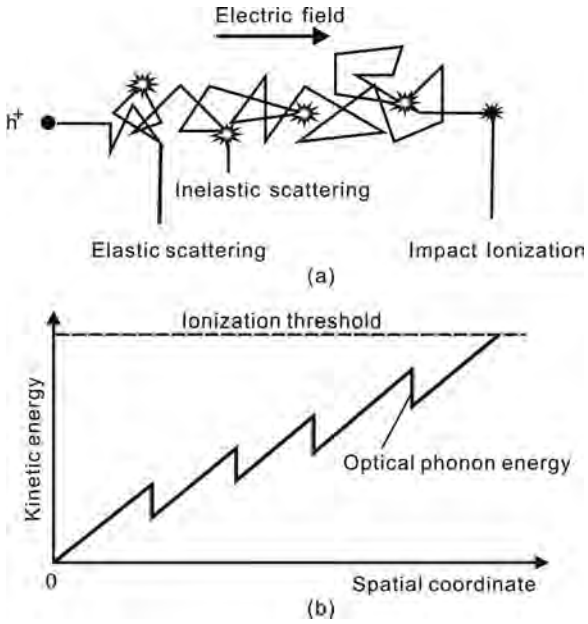

FIG. 5. (a) Schematic representation and (b) energy diagram of the lucky-drift model of an amorphous semiconductor, where a conducting charge carrier h^+ is accelerated by the electric field, while it is subjected to elastic and inelastic scattering, until it reaches sufficient energy for impact ionization. Reproduced with permission from O. Rubel *et al*., J. Phys.: Condens. Matter **23**(5), 055802 (2011). Copyright 2011 IOP Publishing.

a phonon cloud.[142] This Coulomb interaction impedes the movement of the carrier, increasing its effective mass and thus decreasing its mobility.[141] In a nonpolar semiconductor, this electron-phonon or hole-phonon coupling results from the lattice polarization induced by the charge carrier and therefore has a short range. In a polar semiconductor, on the other hand, the lattice constituents possess a permanent dipole moment, inducing a long-range correlation between the charge carrier and the lattice response. As such, polar semiconductors are characterized by an additional carrier scattering mechanism, due to polar phonons. The long-range coupling between electrons and longitudinal optical phonons, known as the Fröhlich interaction, presents a major challenge in charge transport computation for polar materials.[143] Very recently, however, the electronic properties of polar semiconductors have been successfully deduced in a few independent *ab initio* computational studies based on density functional perturbation theory, with clear consistency between the studies and good agreement with available experimental data.[143–145] For this purpose, the electron-phonon coupling matrix elements were split into short-range and long-range contributions, for which two separate mathematical models were employed. The computational results revealed electron scattering by polar phonons as the main relaxation mechanism at low excitation energies, but, interestingly, the dynamics of highly energetic charge carriers were dominated by the interaction with acoustic phonons.[143,145] Accordingly, the polar nature of a dielectric material only seems to have a minor effect on the mobility of hot electrons and holes. The application of the lucky-drift model for polar semiconductors is therefore justified without explicitly taking the dielectric polarity into account. Note, however, that the aforementioned computational studies only considered crystalline semiconductors, i.e., GaAs and anatase TiO_2, so the extrapolation of this idea to amorphous polar materials has yet to be validated.

Zhu *et al*. simulated the breakdown behavior of amorphous SiO_2 by means of classical molecular dynamics in conjunction with tight-binding quantum chemical molecular dynamics. Interestingly, they found a lower band gap of the material under influence of a very high external electric field, ascribed to the loss of the original material structure.[146] Figure 6 shows how the top of the valance band (HOMO) and the bottom of the conduction band (LUMO) start to overlap during the structural reorganization. More specifically, the electric structure shifted from insulator to conductor when the electric field reached a value of 5×10^{10} V/m (see Table I). Since this substantially exceeds the commonly accepted experimental value of 1×10^{9} V/m for amorphous SiO_2 breakdown,[147] Zhu *et al*. performed additional simulations with the inclusion of hydrogen and oxygen defects in the semiconductor. The results showed a faster shift towards

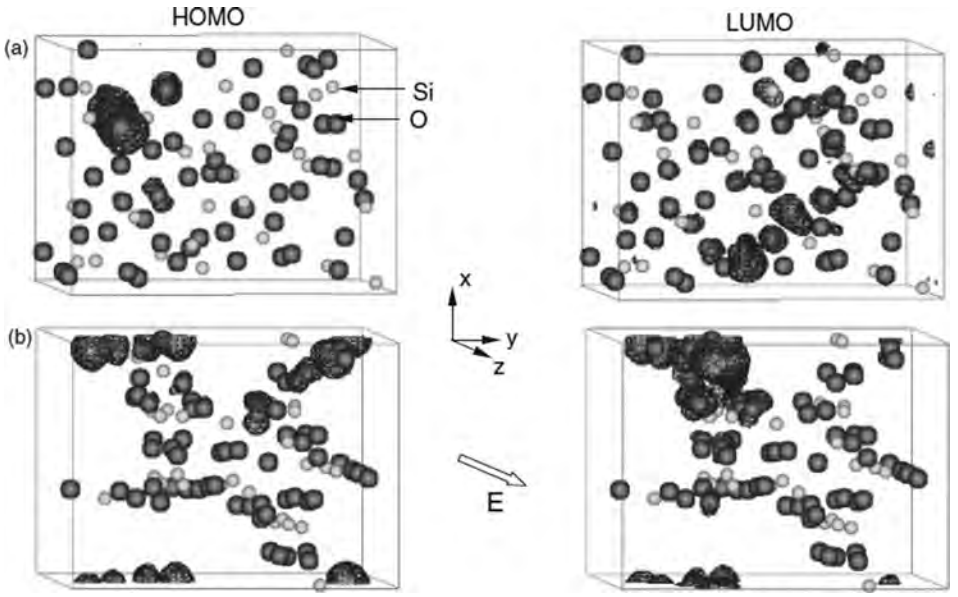

FIG. 6. Spatial probability density distribution (represented by the orbitals) of the highest occupied molecular orbital (HOMO) and the lowest unoccupied molecular orbital (LUMO) in amorphous SiO_2 (a) in the absence of a field and (b) under an electric field of 5×10^{10} V/m along the z-axis. Note how the material reorganizes its structure (compare top and bottom pictures), as well as how HOMO and LUMO become more delocalized and overlap each other in the presence of the field (compare left and right pictures). Reproduced with permission from Z. Zhu *et al*., Jpn. J. Appl. Phys., Part 1 **46**(4S), 1853 (2007). Copyright 2007 The Japan Society of Applied Physics.

TABLE I. Effect of electric field on the band gap of amorphous SiO_2. Reproduced with permission from Z. Zhu *et al.*, Jpn. J. Appl. Phys., Part 1 **46**(4S), 1853 (2007). Copyright 2007 The Japan Society of Applied Physics.

Electric field ($\times 10^{10}$ V/m)	0	1	2	3	4	5
Band gap (eV)	7.5	7.3	6.5	4.8	1.6	0

metallic behavior under the electric field. As such, interstitial defects were concluded to trigger electrical breakdown in amorphous SiO_2.[146] In a recent review by Prasai *et al.*,[148] more detailed information can be found on the electrical behavior of amorphous semiconductors and their modeling by molecular dynamics simulations.

Before extrapolating the above concepts of the band gap theory and lucky-drift model to liquids, one needs to take the influence of their flowing nature into account. On very long time scales, striking differences in lasting effects are seen. Among solid and liquid dielectric insulators, only the first one presents the disadvantage of ageing towards irreversible breakdown, due to the permanent formation of tree-like structures (arborescence) and oxidative degradation under influence of radiation (electroluminescence).[125] Clear differences are also seen on microsecond time scales, where diffusion, convection, ionic drift, chemistry, cavitation, and evaporation play a prominent role in liquids. These processes, which can underlie the bubble mechanism, are unique to liquids and are therefore not expected in solids without a preceding melting step. On the time scales of nanoseconds or picoseconds, however, charge transport by heavy particles becomes less important. Hence, which significant differences between liquids and amorphous solids can we expect in such short time intervals that can account for dissimilar electrical behavior?

The answer might—or might not—be electron solvation. Excess electrons in a liquid influence the surrounding solvent molecules by their Coulomb interaction, in a very similar manner as charge carriers in a solid semiconductor or insulator (see above). Since liquid molecules are more mobile than their solid counterparts, this polaronic effect is more pronounced in liquid media. This is especially true for polar solvents, such as water, where a structured shell of solvent molecules is rapidly formed around ionic solutes—or in our case around excess electrons. Therefore, in clear association with the liquid semiconductor model, excess electrons in polar liquids can be located either in the conduction band or trapped states in the band gap of the solvent, corresponding to a quasi-free or solvated electron, respectively. The transition of a quasi-free electron towards a trapped state is called electron solvation. The lifetime of quasi-free electrons in water, for instance, is less than 1 ps, according to measurements and molecular dynamics simulations.[149–151] Figure 7 depicts a semiclassical interpretation of the solvation dynamics, where a conduction band electron first gets trapped at a weakly H-bonded OH group and subsequently decays to its stable solvation state. The fast solvation dynamics has formed the base of a second influential criticism on the electronic mechanism. Namely, excess electrons in polar liquids are argued to be solvated before they reach sufficient energy

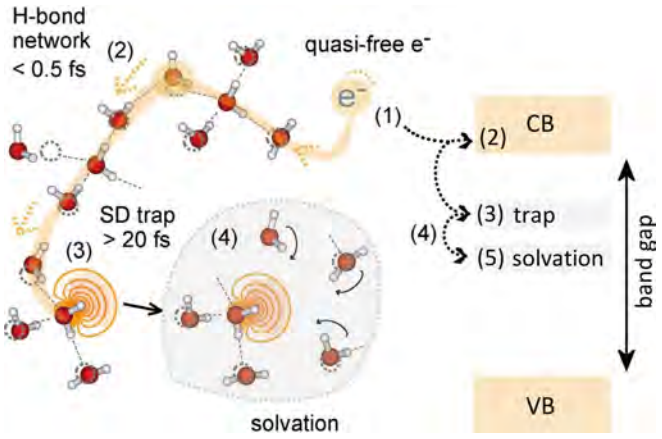

FIG. 7. Schematic representation of electron solvation in water: (1) and (2) a quasi-free electron in the conduction band (CB) is transferred on attosecond timescales along the H-bond network with an extremely fast hopping rate, (3) until it gets trapped in a localized state at a weakly H-bonded OH group of a single donor (SD) water species, (4) followed by electron solvation dynamics, (5) to reach the solvated electron state. Adapted with permission from D. Nordlund *et al.*, Phys. Rev. Lett. **99**(21), 217406 (2007). Copyright 2007 The American Physical Society.

to ionize liquid or solvated molecules (see, e.g., Refs. 45–47, 49, 51, and 57). This argument is, however, based on the conjecture that this short lifetime is persistent in high local fields, while the electronic features of water are known to be altered under such conditions (see Sec. II E). Moreover, the quasi-free electron lifetime is locally extended in the presence of a large number of excited electron states, an effect observed in Ref. 151 and attributed to the saturation of pre-existing trapping states.

To understand the field effect, consider the semiclassical model for electric field-induced ionization of a neutral molecule, as depicted in Fig. 8(a). For field strengths below the ionization threshold, the positive core of the molecule will be pulled in the direction of the field and an electron in the molecule will be pulled in opposite direction, creating a dipolar molecule. Increasing the field will result in further excitation until the electron is eventually extracted from the molecule, creating an ion and a free electron. During this process, the positive core of the transient dipolar molecule can be considered rigid. The process can also be explained with a decreasing potential barrier for the electron in the potential well of the molecule until tunnel ionization occurs, as shown in Fig. 8(a). Let us repeat this process for a solvated electron in water. Based on molecular dynamics simulation, the structure of this electron is generally represented as an electron surrounded by a cage of six water molecules (Fig. 9), whose dipolar moments are directed in such a way that the electron is stabilized and that the potential energy of the system including the neighboring water molecules is minimized.[153] For reasons of simplicity, we assume that the water molecules in the semiclassical model are rigid, while they are able to rotate. When a weak external electric field is applied, the electron is pulled in the opposite direction of the field [Fig. 8(b)]. The dipolar moments of the water molecules, on the other hand, will partly align with the field, making the molecules rotate. Upon this rotation, they cannot attract the electron as much as before, resulting in a stronger

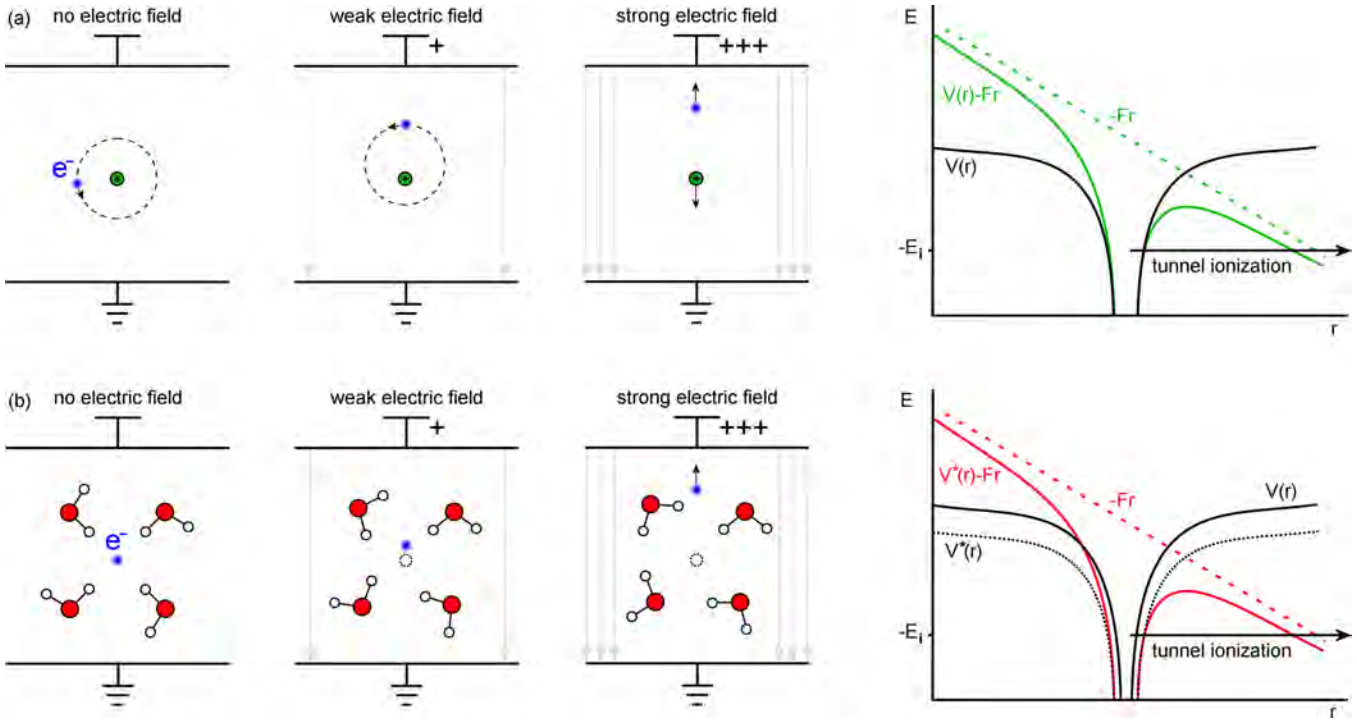

FIG. 8. (a) Field-induced ionization of a neutral molecule in vacuum and (b) field-induced desolvation of a solvated electron in water, represented by (left) a semiclassical model and (right) an energy diagram. In (a), the positive core of the molecule is indicated in green. In (b), oxygen atoms are depicted in red, hydrogen atoms in white and the initial central location of the electron is shown as a dotted circle. In the energy diagrams, $V(r)$ is the potential well of the electron with energy E_i without external field. (a) When an external field F is applied, the electron in the neutral molecule experiences a potential $V(r) - Fr$. For sufficiently high field, the potential barrier is decreased enough to make the electron tunnel away. (b) The situation is different for a solvated electron in an external field, since the surrounding water molecules rotate under influence of the field. The rotation makes the potential well generated by the water molecules broader and shallower, represented in the energy diagram by $V^*(r)$. Adding the contribution of the field gives $V^*(r) - Fr$, resulting in a stronger potential barrier decrease as compared to (a).

destabilization and delocalization of the electron. Meanwhile, other water molecules in the opposite direction of the field will also partly align with the field, attracting the electron with their positive pole, causing even more electron destabilization and delocalization. Further increase in the field will eventually result in a quasi-free electron. This mechanism is clearly very different from the first mechanism of the electron in the neutral molecule. As explained in the caption of Fig. 8, this results in a faster decrease in the potential barrier for the electron and thus earlier tunnel ionization as compared to field ionization from a molecule with the same binding energy. In terms of the semiconductor model of water, the increasing external field results in a narrowing band gap. Note the consistency with the results from Zhu *et al.* for the case of amorphous SiO_2 mentioned above, where a narrowing band gap and a loss in material structure were found as well. Analogously, water can lose its original structure under influence of a field. Based on this thought experiment, one can argue that the lifetime of quasi-free electrons is prolonged in a high electric field.

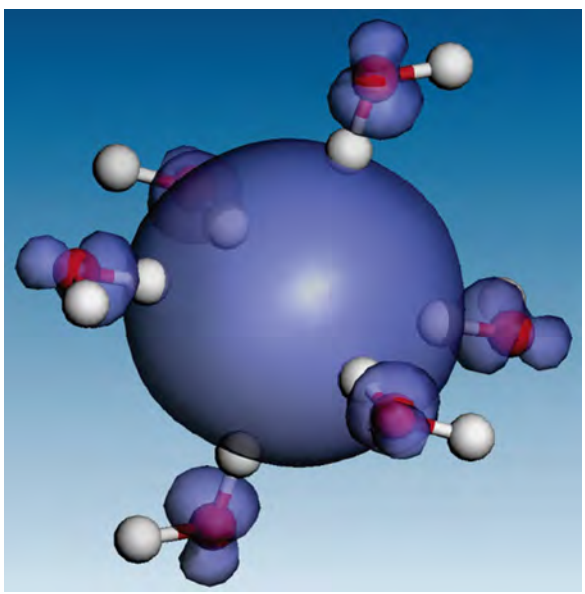

FIG. 9. Kevan structure for the solvated electron in water, calculated for six stabilizing water molecules. The blue orbitals represent the electron probability density. Reprinted with permission from J. Zhao *et al.*, Chem. Rev. **106**(10), 4402–4427 (2006). Copyright 2006 American Chemical Society.

Additionally, this analogy and thought experiment have important implications on both the lifetime and mobility of solvated electrons. Under standard conditions in the absence of an external field, the lifetime of a ground-state solvated electron in pure water ranges in the microsecond regime.[154,155] In low electric fields, its movement through the liquid is limited by the surrounding shell of solvent molecules that it drags along. This explains why solvated electrons have a similar mobility as ions in polar liquids, whereas in nonpolar liquids, their mobility is generally several orders of magnitude higher in comparison to ions in the same medium, as well as to electrons in polar solvents.[156] In

strong electric fields, however, the polar solvent molecules of the solvation shell will align along the field with their dipole moment, and the shell structure of the solvated electron will disappear, enabling the electron to move with higher mobility. Since a fast electron is harder to catch than a slow one, it should also have an extended lifetime.

More accurate *ab initio* molecular dynamics simulations and experiments are required to confirm these field effects for aqueous electrons. The model of Fig. 9, although useful, likely oversimplifies the situation, since the solvated electron structure is still under debate. In Ref. 157, two types of solvated electrons were detected with different vertical binding energies. Recently, multiple configurations have been proposed,[158,159] where the localized electrons can occupy a cavity or a non-cavity region with higher water density.[149,160,161] Next to that, a solvated electron might be stabilized by a neighboring positive counter-ion.[158] Remarkably, quasi-free electrons in amorphous ice have a similar lifetime as in liquid water,[162,163] suggesting that electron solvation might not be so different in liquids and amorphous solids after all. Considering these complications, the solvated electron structure and its solvation dynamics in an external electric field are likely even more complex.

The experimental investigation of excess electrons in a liquid in a static field, for instance right below the threshold for plasma formation, can be performed with similar methods as applied in the absence of an external field. In these methods, the excess electrons are usually generated by means of radiolysis[164–167] or laser-induced ionization[150–152] with short beam pulses. The produced solvated or quasi-free electrons can be measured with synchronized optical methods, such as pump-probe transient absorption measurements,[159,168] time-resolved resonance Raman spectroscopy,[159] transient terahertz spectroscopy,[150] core-hole decay spectroscopy,[152] and the time-resolved optical interferometric technique described in Ref. 151, as well as steady-state or time-resolved electron paramagnetic resonance spectroscopy.[169,170] The latter two techniques are able to detect solvated electrons in the form of radical pairs or radical-ion pairs, due to interaction with co-existent radicals or ions in the solution.[169,170] In addition, alternative methods have been described in literature to measure solvated or quasi-free electrons exposed to an external field in a less direct manner. A first example is explained in Ref. 171, where solvated electrons are observed by electrical characterization, by injecting electrons from a metal electrode into water layers on silica gel particles under high voltage application. As a second example, both aqueous and nonaqueous reactions of excess electrons ejected from a submerged oxide-coated cathode can be studied by means of cathodic hot electron-induced electrogenerated chemiluminescence, a relatively novel technique, reviewed in Ref. 172. In order to measure excess electrons generated before or during voltage-induced plasma formation in the liquid phase, the most appropriate and unambiguous procedures will probably exert a time-resolved optical detection method synchronized to the applied voltage pulse. For this purpose, inspiration can be found in the various detection techniques utilized in experimental studies of the solvated electron, as well as laser-induced breakdown in liquids. Alternatively, indirect detection methods can be considered, where excess electrons are scavenged or converted to more stable species, which on their turn can be detected by means of a complementary technique, such as electron paramagnetic resonance or fluorescence spectroscopy. A spin trapping method for solvated electrons is, for instance, proposed in Ref. 173. This approach is similar to the chemical probe-based diagnostics for other reactive species in the liquid phase, as discussed in Ref. 40. Nonetheless, in order to avoid dubious measurements with such technique, the selectivity of the used probe to other plasma-induced reactive species needs to be scrutinized.

In summary, the above insights advocate an amorphous semiconductor model for liquids, especially on nanosecond time scales and below. On these time scales, excess electrons in the liquid can decay from the conduction band towards localized states in the band gap through fast solvation dynamics associated with reorientation of water molecules. There is, however, a clear need to investigate the solvation dynamics in the presence of strong electric fields and a large number of excess electrons, since this has not been investigated in literature, to our knowledge.

C. Bubble mechanism: The existential crisis of nanobubbles

Bubbles appear deceivingly simple phenomena. With a closer and more critical look, however, many complexities boil to the surface. From the vast variety in bubble shapes and oscillation modes to the enigmatic zigzag and spiral rising paths,[174,175] this peculiar hydrodynamic curiosity has spawned an overflowing library of scientific reports with relevance to biology, chemistry, engineering and many more disciplines.[174,175] Despite the substantial research efforts, many aspects of fundamental bubble behavior remain speculative. In the light of in-liquid plasma initiation, the possible mechanisms for bubble nucleation, with boiling, in particular, are clearly some of the most relevant aspects. Homogeneous nucleation, which occurs under controlled thermodynamic conditions, is likely unimportant in this context. Heterogeneous bubble nucleation, on the other hand, can generally have many triggers, including contamination, liquid chemistry, and radiation,[176] which are abundant in plasma-liquid interactions.

For in-liquid plasma initiation experiments and applications, contamination can be naturally present in the form of nanoparticles (see Sec. II D), small gas pockets, or a combination of both. Depending on their size, gas pockets are classified as macrobubbles (over 1 mm), microbubbles (over 1 μm), and nanobubbles (below 1 μm), which display distinct behavior, as explained in Fig. 10(a). Studies and discussions on in-liquid plasma initiation were limited up to now to macrobubbles and microbubbles (see, e.g., Refs. 42, 45–49, 51, and 57) whereas the concept of random pre-existing nanobubbles has only been alluded to in some reviews,[45,47] without further elaboration. Clearly, the relevance of this topic is still unexplored in the field.

Nanobubbles are generally recognized in scientific literature as gas cavities with dimensions up to 1 μm[179,180] and can be present in the bulk liquid or at a submerged surface [Fig. 10(b)]. According to the classical thermodynamic

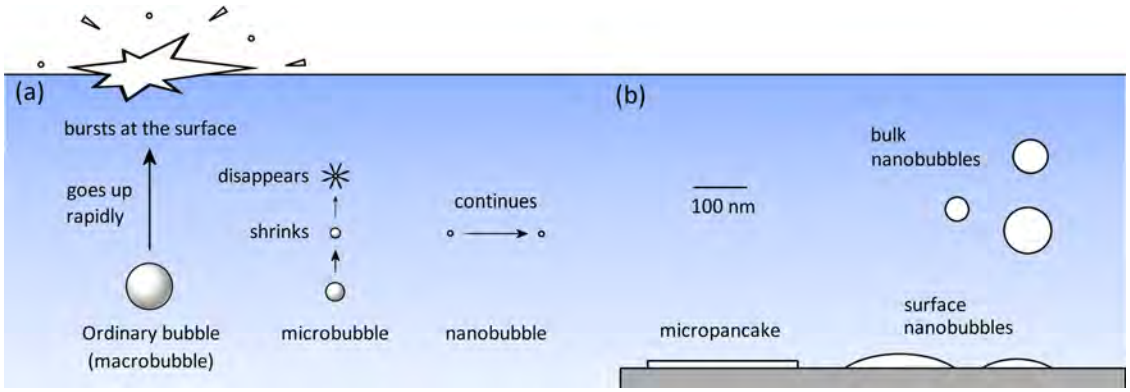

FIG. 10. (a) Comparison of a macrobubble, which rapidly rises due to its buoyancy, a microbubble, which slowly rises and shrinks due to its surface tension, and a bulk nanobubble with high stability, whose movements are governed by Brownian motion. (b) Comparison of bulk nanobubbles, which occur in the bulk liquid, and surface nanobubbles, which are present at a submerged surface, with a micropancake as a special example. Figure (a) is adapted with permission from M. Takahashi *et al*., J. Phys. Chem. B **111**(6), 1343–1347 (2007).[177] Copyright 2007 American Chemical Society. Figure (b) is adapted with permission from J. R. Seddon *et al*., ChemPhysChem **13**(8), 2179–2187 (2012).[178] Copyright 2012 John Wiley and Sons.

theory, they should not exist due to their high internal pressure, resulting from their strong surface tension, as explained in Fig. 11.[179–181] If the internal pressure is not in balance with the degree of gas saturation in the surrounding liquid, the bubble gas should dissolve into the liquid, making the bubble smaller down to complete dissolution. The internal pressure of nanobubbles is, however, anomalously high, since an unrealistic supersaturation degree of the liquid would be required to ensure their existence. Yet, stubborn as they are, they do exist. Stable bulk nanobubbles were first reported in 1982 by means of sonar display,[182] while the reality of stable surface nanobubbles was postulated in 1994, based on force measurements between hydrophobic surfaces immersed in aqueous solutions.[183] Their gaseous nature was not proven until 2014[184] and 2015,[185] explaining why they have only recently been recognized by the scientific community. They are considered stable, with observed lifetimes up to several days[178,180] or even weeks.[186] Multiple theories have been proposed to explain their stability, as discussed in Refs. 180 and 187, but substantial evidence in favor of one theory is still lacking.

Nanobubbles have been detected in natural waters[182] and are generally believed to be widespread in the environment, but a detailed study on their occurrence is yet lacking. As suggested in Ref. 187, experimental protocols might unintentionally promote their formation in laboratory solutions, where they can be generated by means of acoustic, hydrodynamic, mechanical, optical and particle cavitation, as well as chemical and electrochemical reactions.[189–192] Note that these processes are prevalent in a plasma-liquid environment, hence an increased number density can be expected. The mechanisms apply to both bulk and surface nanobubble production, but the exact preparation procedures differ. Bulk nanobubble generation generally involves mixing of gas into the liquid, whereas surface nanobubbles are standardly prepared by a solvent exchange process (compare, e.g., Refs. 189 and 190). Besides that, it has been speculated that nanobubbles are constantly created by cosmic radiation.[178] Literature often suggests that they can only occur in supersaturated gas solutions[187] and that their cavitation is only related to pressure gradients and variations, contrary to temperature change,[192] yet this is opposed by experimental and theoretical reports.[189,193,194] While most research on this topic is performed with water, nanobubbles have also been reported for aqueous ethanol solutions[195] and protic non-aqueous solvents.[196]

Bulk phase nanobubbles can be as small as 10 nm in diameter,[179] but typical sizes range between 100 and 300 nm.[179,197–200] Various solution preparation methods generally lead to number densities between 10^{12} and 10^{15} m^{-3},[197–200] although values up to 1.9×10^{19} m^{-3} have been obtained.[186] Detection techniques include light scattering,[184] cryoelectron microscopy,[201] and a resonant mass measurement method that can distinguish the bubbles from liquid emulsion or solid nanoparticles.[202] Due to their small dimensions, nanobubbles have a negligible rising velocity compared to Brownian motion in the liquid.[192] This feature stands in contrast with microbubbles, which slowly rise

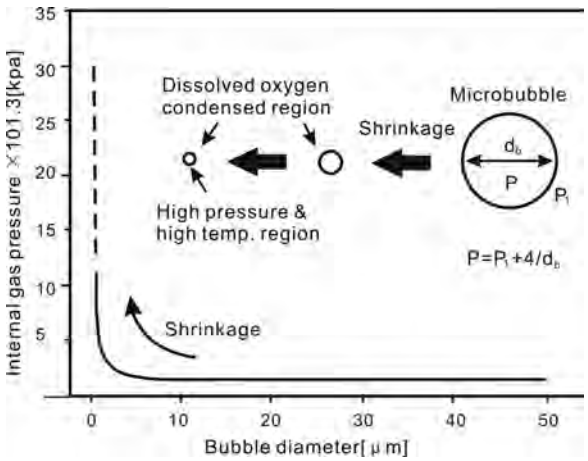

FIG. 11. Evolution of the internal gas pressure during shrinkage of a nanobubble in liquid at standard conditions according to the formula $P = P_1 + 4/d_b$ from standard theory, where P is the internal bubble pressure, P_1 is the liquid pressure at the bubble depth location, and d_b is the bubble diameter. For d_b below 1 μm, the internal pressure becomes so high that the bubble should dissolve into the liquid, in disagreement with experiments. Reprinted with permission from P. Li *et al*., Chemosphere **77**(8), 1157–1160 (2009).[188] Copyright 2009 Elsevier.

towards the surface. Interestingly, nanobubbles generally have a negative surface charge according to theoretical and experimental evidence,[192,197,203–205] although this might depend on solution pH.[187] The negative charge results in an outwards repulsive force on the surface, counteracting the high surface tension. Correspondingly, specialized literature sometimes uses the term *bubstons*, which is short for ion-stabilized nanobubbles.[197] Negative nanobubbles are strongly attracted to a neighboring high voltage anode, while repelled by a cathode, and might therefore be responsible for the reported polarity effects in voltage-induced in-liquid breakdown (see Sec. II A). Close to the electrode surface, they cause tremendous electric field enhancement, as shown by the simulation results in Ref. 206, which facilitates plasma initiation. Additionally, they can play a key role in streamer branching, in agreement with the simulation study[91] on the interaction of streamers with inhomogeneities. As such, this mechanism can explain the polarity dependence of streamer branching.[46] The importance of nanobubbles in laser-induced breakdown of water has already been illustrated by a few experimental studies. Indeed, in 2006, Bunkin and Bakun were the first to demonstrate plasma initiation in nanobubbles as a seed mechanism for the optical breakdown of water, for laser intensity below the optical damage threshold of the solvent.[207] More recently, their group used the technique to assess nanobubble properties, such as their number density, as illustrated by Fig. 12.[197,203] Ikezawa *et al.*, on the other hand, applied argon nanobubbles to enhance the optical sensitivity of laser-induced breakdown spectroscopy.[208]

Surface nanobubbles have the shape of a spherical cap, with a height in the order of 1 to 10 nm and a width of about 100 nm[187,194] or around 1000 nm,[180,194] where the latter are sometimes called *micropancakes* [Fig. 10(b)]. Their contact angle with the surface differs significantly from what would be expected of macroscopic bubbles. They are preferably formed on hydrophobic, rough surfaces,[209] but also occur on hydrophilic substrates.[210–212] According to a popular school of thought on their stability, the three-phase contact line is fixed on the substrate by a strong pinning mechanism. Some scientists have even used the term superstability, since the surface bubbles do not seem to be affected by shockwaves[213] and temperatures near the boiling point of water.[214] The proposed pinning mechanisms and other stability theories are reviewed in Refs. 181 and 180, respectively. Another review in Ref. 215, with high relevance to voltage-induced in-liquid plasma initiation, has investigated how an applied voltage on the substrate influences the surface properties. According to the findings, a higher surface charge density results in smaller and more surface nanobubbles, a smaller slip length and a larger drag of liquid flow. Also this type of nanobubbles is thought to be negatively charged.[187] Next to that, theory demands that they are subjected to continuous convection (see Fig. 13). As they can play an important role in voltage-induced breakdown experiments, future research needs to point out the possibility to have a nanobubble attached to the pin electrode tip. An overview of all detection methods and other related information can be found in Ref. 189.

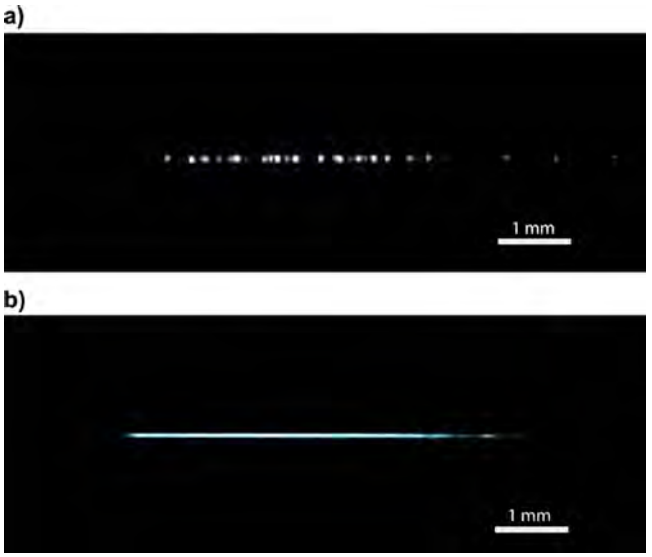

FIG. 12. Optical breakdown patterns from a horizontal laser beam (a) in degassed NaCl solution, with a low number density of nanobubbles, and (b) in the same solution after 24 h exposure to the open atmosphere, where the density has increased, as easily deduced from the continuous and brighter emitted light. Reprinted with permission from. N. F. Bunkin *et al.*, J. Phys. Chem. B **120**(7), 1291–1303 (2016). Copyright 2016 American Chemical Society.

In a nutshell, the role of bulk and surface nanobubbles in in-liquid plasma initiation and propagation processes is left vastly unexplored. A few first studies have been performed in the context of laser-induced breakdown of liquids, whereas studies on voltage-induced breakdown have yet solely been centered around micro- and macrobubbles. Given the expected contribution of inhomogeneities of the liquid in these processes, we want to motivate experimental research on this highly relevant topic.

D. Interface mechanism: Through the eye of the needle electrode

In normal conditions, every metal is covered with a naturally grown oxide layer. The thickness of the oxide layer is strongly dependent on the metal type, the surrounding

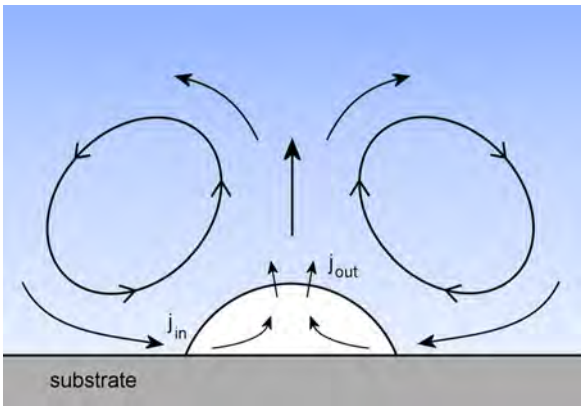

FIG. 13. Convection processes in and around a surface nanobubble according to the dynamic equilibrium theory of Refs. 216 and 217. The gas outflux j_{out} at the bubble surface is driven by the surface tension and compensated by a gas influx j_{in} at the contact line.

environment, temperature and the time of exposure to the environment. It usually ranges between 1 and 100 nm,[218–223] but values up to 50 μm have been reported for growth in strongly oxidative environment.[224–226] In water with strong oxidative chemistry, as during plasma treatment, thick and fast growing oxide layers can be expected on metal electrodes. In other liquids, different types of layers are formed through analogous processes, as, e.g., nitride layers in liquid nitrogen and carbon enriched layers in hydrocarbons, under influence of reactive nitrogen species and carbonaceous species, respectively.[227] In hydrocarbons, liquid conversion by electropolymerization has also been suggested as a layer deposition mechanism.[218] During this growth process, defects and impurities are included into the layer. As a result, the layer can contain small cavities with lower dielectric constant, for instance from interaction of nanobubbles with the interface. Plasma initiation is favored in such cavity due to its lower breakdown strength and the electric field distribution along the nanolayer, in analogy with the bubble mechanism of Sec. II C. Electrical breakdown of the cavity gas can lead to a significant pressure increase in the cavity and local thermal instabilities, erosion and chemical degradation in the cavity surface, in agreement with the erosion mechanism for solid breakdown described in Ref. 1. Consequently, a crack can be formed or the plasma can penetrate through the nanolayer towards the liquid. This process is obviously faster and more effective for cavities located closer to the nanolayer-liquid interface. Once the plasma reaches the liquid, the local electric field near the liquid interface is enhanced and a streamer head will be formed.

Hence, we hereby propose a third class of theories on plasma initiation in liquids, where streamer inception in the liquid phase is assumed to be preceded by plasma initiation in the electrode-liquid interface. This class will be further referred to with the term *interface mechanism*. To our knowledge, only one example of this mechanism has been postulated before in literature. In his reviews,[228,229] Mesyats advocates the occurrence of microexplosions at a metal electrode submerged in a dielectric liquid, as an effect of short energy concentration in a microvolume of the electrode. Such microexplosions, also called explosive centers or ectons, have been thoroughly studied in the context of explosive electron emission from a cathode in vacuum arcs, where the process is favored at metal electrodes with dielectric inclusions or covered by a dielectric layer.[230] Although Mesyats only gives a short, qualitative account of the phenomenon for in-liquid discharge and does not explicitly propose it as an initiation mechanism, it can be interpreted as one. The mechanism is reminiscent of the low-macroscopic-field electron emission from dielectric films, as explained with the local field enhancement hypothesis in the review,[231] as well as the breakdown mechanism for solid amorphous dielectrics described in Ref. 1. The former accentuates that thin dielectric films should be seen as "hopping conductors" instead of semiconductors, in agreement with the latter.

Conditions of thermal instability can be met, since the conductivity of the oxide nanolayer might increase with temperature and since its temperature rises by conduction currents and dielectric losses due to polarization. At sufficiently high local electric fields, the rate of internal heating can no longer be compensated by external cooling effects, and thermal breakdown of the nanolayer will occur. Depending on the nanolayer and liquid properties, these conditions for thermal instability are favorable at specific locations. First of all, this mechanism is promoted by local electric field enhancement at the layer-liquid interface by sharp electrode curvature and by foreign particles or bubbles. Second, strong variations in thickness or imperfection density of the nanolayer can give rise to a local narrow current density maximum with high amplitude. If the nanolayer has significantly higher resistivity than the surrounding liquid, for instance, a narrow minimum in nanolayer thickness is expected to have increased current density. Imperfections in the nanolayer structure, on the other hand, may act as traps for free electrons. Accordingly, they create energy levels that lie just below the conduction band of the nanolayer (see Fig. 14), promoting conductive currents through an electron hopping process.[1,220] Figure 14 is reproduced from the work of Lewis,[218] which is an old but still recommended source on the detailed electronic description of a metal-oxide-liquid junction. In this context, it is very interesting to note that Lewis proposed streamer initiation by the combination of two related mechanisms in his later work.[232] One mechanism concerns the Lippmann effect in which the electric fields of the double layers at the electrode diminish the interfacial tension, inducing a region of low density on the electrode surface. The other is the Auger effect in which electrons obtain high energy from electron-hole recombination across the large energy gap, allowing impact ionization. Apart from that, an elastically deformable nanolayer can additionally undergo electromechanical breakdown, when it is subjected to electrostatic compression forces that exceed its mechanical compressive strength.[1] The latter nanolayer breakdown processes will be associated with shockwave generation and cavitation, which allows plasma initiation in a similar way as in the bubble mechanism (see Sec. II C). A 2D model for cavitation as an effect of an underwater explosion near a wall is described in Ref. 227.

The influence of suspended solid particles on the breakdown mechanism has frequently been investigated in research on commercial transformer oils, where solid impurities are present as fibers or as dispersed solid particles.[1,233] To our knowledge, this particle mechanism has not been proposed before as plasma initiation process in pure liquids, for the obvious reason that such liquids are not expected to contain significant impurities. Nevertheless, it should be taken into account here as well, since in-liquid plasma can introduce considerable amounts of solid particles into the liquid phase, either as an effect of electrode erosion or by chemical synthesis. Electrode erosion occurs through various mechanisms, depending on the stage of plasma evolution. Before breakdown, material of the electrode where plasma is initiated can be transferred towards the liquid as an effect of electrode melting and evaporation, whereas the counter electrode or opposing wall can be eroded by the striking shock wave coming from the approaching streamer head.[227] Accordingly, erosion effects are even important for low energy pulsed corona in liquid, as observed in Refs. 220, and 234–236. Figure 15

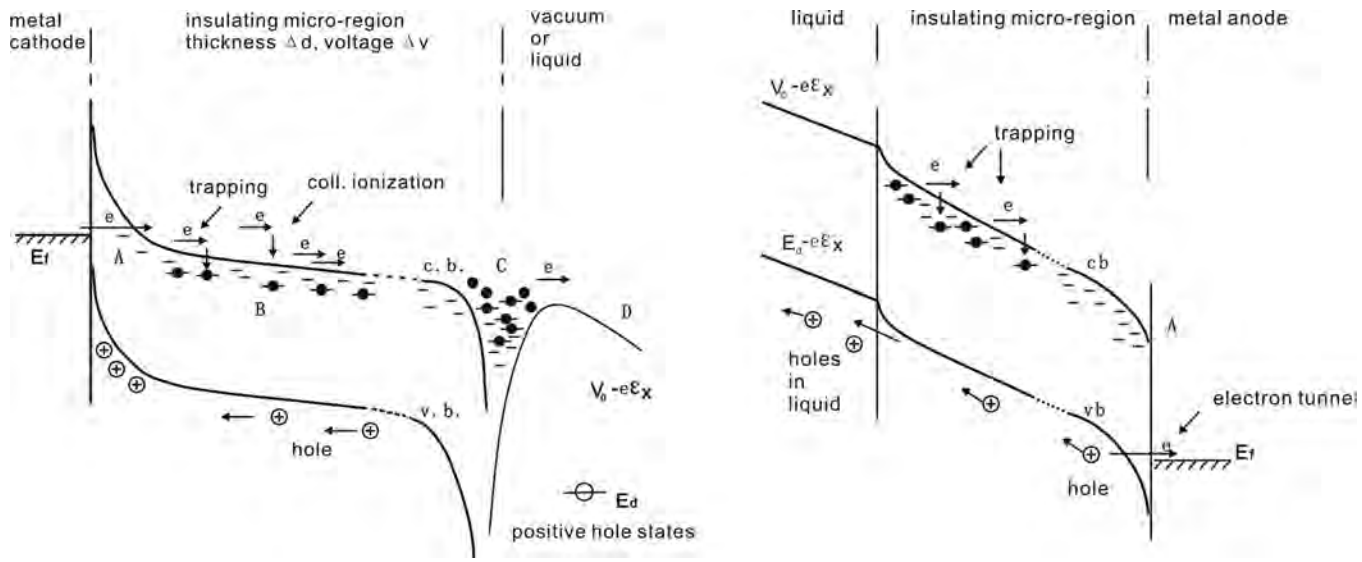

FIG. 14. Electron tunneling and hole drift mechanisms in a metal-oxide-liquid junction during voltage application (left) at a metal cathode and (right) at a metal anode, according to T. J. Lewis *et al*. When the applied voltage increases, the potential barrier in between the metal cathode and the oxide layer is lowered, until electrons can tunnel towards the conduction band of the oxide. There, collisional ionization and trapping processes bring the electrons in shallow trapped states, from which they can escape by thermal activation towards the conduction band or tunneling towards neighboring states. This hopping mechanism forms the basics of current conduction in the oxide layer. At the anode, the situation is analogous, but electrons tunnel towards the anode from the valance band in this case, generating holes. From Lewis, *The Liquid State and its Electrical Properties*. Copyright 1988 Springer. Adapted with permission from Springer Nature.

illustrates this for tungsten and titanium needle electrodes. During breakdown, metallic liquid wells are formed at the contact points between the plasma channel and the electrodes. These molten wells are subjected to numerous forces, originating from the adjacent pressure and temperature gradients and, in the case of high currents, from magnetic spinning as well. These forces are symmetric at both electrodes and dominate molten droplet emission. This explains why electrodes of identical material are eroded almost independently of polarity during this stage. After the discharge is turned off, further electrode erosion can occur in the form of cracks and thermal spalling. A more detailed description of these processes in function of the discharge stage is found in the review of Belmonte *et al*.[227]

From these insights, the extent of electrode erosion is evidently strongly dependent on the melting point and composition of the electrode material. Lukes *et al*. confirmed this for underwater corona by comparison of three needle electrode materials.[235] In the latter study, however, electrolysis was found to have a large contribution to the total erosion as well, in particular for the stainless steel needle, which released up to 40%–50% of its eroded material in the form of iron ions. For a given electrode material, the composition, shape, size and number of generated nanoparticles can be controlled with several parameters, including the discharge duration, pulse energy, electrode shape and liquid properties.[227] Pulsed underwater corona from a needle electrode, for instance, leads to higher erosion rate at higher water conductivity and larger

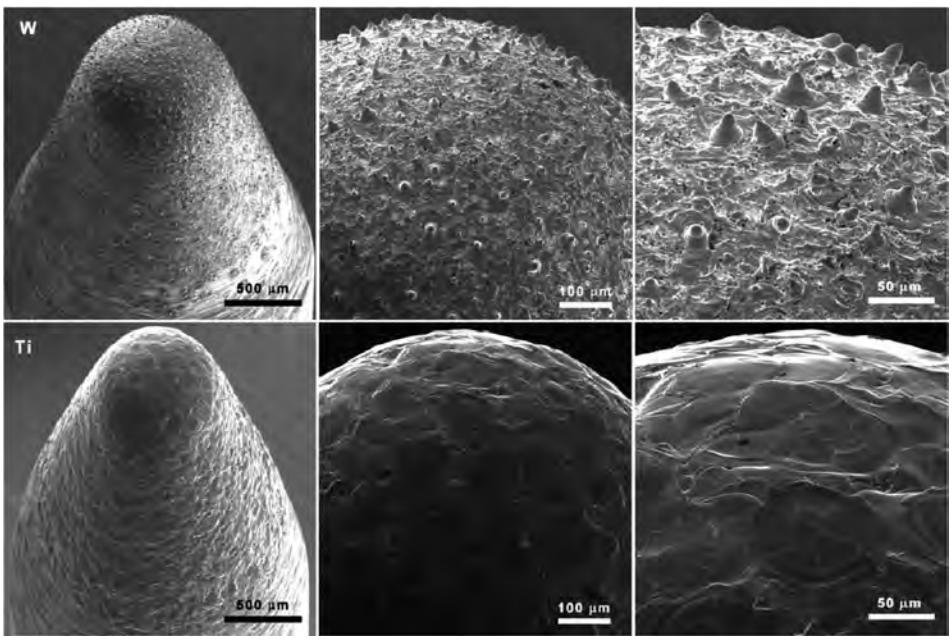

FIG. 15. SEM images of eroded tungsten (upper panels) and titanium (lower panels) needle electrodes tips after 40 min operation in a pulsed in-liquid corona plasma reactor, for different magnifications. Note that the corona discharge remains located at the electrode and does not reach the opposing electrode, so the electrical current remained fairly small during the experiment. Reproduced with permission from P. Lukes *et al*., Plasma Sources Sci. Technol. **20**(3), 034011 (2011). Copyright 2011 IOP Publishing.

needle diameter.[234,235,237] Nanoparticles can also be chemically synthesized by conversion of the liquid[238] or dissolved ions.[239] As should be noted, electrode erosion as well as liquid conversion by means of plasma can produce nanoparticles with complex shapes, including homogeneous colloids, nanotubes, nano-onions, nanohorns, etc., and further clustering of these particles can occur.[227,238] Similarly to the solid impurities in commercial transformer oil, plasma produced nanoparticles can move towards regions in the liquid with locally high electric fields and influence plasma initiation and propagation. As a main difference, these particles do not have to be dielectric (e.g., metal oxide nanoparticles), but can also be metallic or composite colloids. Nanoparticles are sometimes applied in laser-induced breakdown of liquids in order to generate nanoplasma in a so-called plasmonic nanobubble, as explained in Fig. 16. This effect has evident resemblance with the injection of highly energetic electrons from irradiated plasmonic nanoantennas, as recently described in Refs. 240–242. Similar plasmonic behavior can be expected during high voltage application for a nanoparticle located near an electrode or for sharp protrusions at an electrode surface, as clearly seen in the upper panel of Fig. 15. In addition to all these effects, heterocoagulation between nanoparticles and nanobubbles has been reported (see Fig. 3 above).[199] The resulting clusters can also contribute to the in-liquid plasma mechanisms.

In summary, the submerged electrodes for voltage-induced plasma initiation are subjected to several effects, including deformation, erosion and oxidation, resulting in roughness and the formation of an oxide layer. These manifestations can lead to several breakdown mechanisms, which have not yet received sufficient attention in research. Additionally, electrode erosion and liquid conversion introduce nanoparticles in the liquid, which can cluster with nanobubbles, forming different types of inhomogeneities in the liquid or on the electrode surface. As such, they are expected to influence plasma initiation and propagation as well.

E. Liquids in strong fields: Can the floating water bridge help us cross the knowledge gap?

Even under standard conditions, the microscopic structure of water remains a mystery.[244] According to the standard model, each water molecule is on average bonded to four others in a tetrahedral pattern.[245] In 2004, a controversial study in *Science*[246] opposed this view, suggesting rings and chains of water molecules, where they would only bind to two others. More recent research indicated an even higher complexity of molecular configuration, where rings composed of six molecules on average form the entity of tetrahedral-like units in a continuous, flexible, hybrid network.[247] Moreover, water is perhaps not purely liquid. Instead, it might be simultaneously liquid and solid in a multiphase arrangement, literally like an ocean stippled with tiny icebergs each comprising about 100 molecules.[244] To make it even more complex, the microscopic structure depends strongly on temperature, pressure and solutes, thus also the acid-base balance.[248–250] As should be reminded, this labyrinthine picture only applies to a confined area near standard conditions in the phase diagram of water. Further exploration of the phase diagram has led to the discovery of sixteen crystalline and three amorphous ice states.[250] Among these controversies, complexities and numerous anomalies of water, researchers seem to agree on one thing—when it comes to water, a lot boils down to the strong hydrogen bond.[244,249,250] A lot, though not everything. Van der Waals interaction has now been revealed as its indispensable sidekick, which should be taken into account in *ab initio* computer simulations to ensure accurate results.[251,252]

For plasma initiation in water, this is just the tip of the iceberg. That is, one is clearly treading on thin ice when standard water properties are extrapolated to a situation with a strong electric field. Indeed, enhanced structuring of water under influence of an external field is a well-known phenomenon in interfacial electrochemistry, where it has been observed in both experiments and molecular dynamics simulations.[253] Nevertheless, caution is required when interpreting results from literature, since they usually are specific for the investigated conditions. At an interface, the local restructuring process also depends on the distance to the surface.[253] Apart from the overall liquid reorganization, ionic solutes break out of their solvation shells at a field strength around 1.5×10^9 V/m, gaining higher mobility.[254] Moreover, salt addition reduces the protonic mobility, as well as the required field for water dissociation.[254] A field of 2×10^9 V/m induces electrolysis of water, resulting in molecular hydrogen production.[255] At the current state of research, the effect of the electric field on hydrogen bonds is not clear, with seemingly contradicting studies.[250]

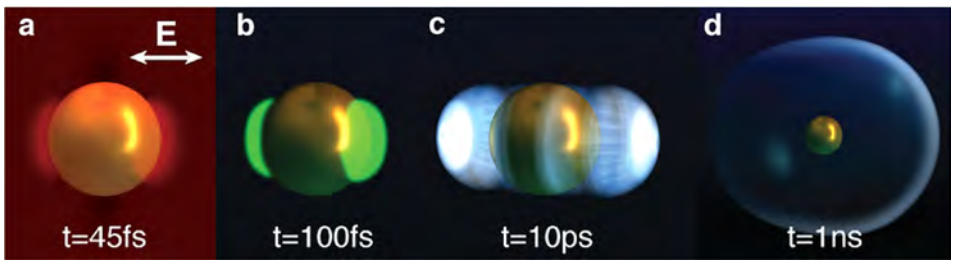

FIG. 16. Schematics showing the formation of a plasmonic nanobubble in water. (a) A metal nanoparticle is irradiated by an ultrafast infrared laser, where the double arrow represents the oscillating electric field. This results in the oscillatory displacement of the conduction electrons in the nanoparticle. (b) The surrounding water is ionized, creating nanoplasma near the poles of the colloid. (c) The water is isochorically heated during the relaxation of the plasma, inducing a pressure wave and thus (d) generating a nanobubble around the particle. Reprinted with permission from E. T. Boulais *et al.*, Nano Lett. **12**(9), 4763–4769 (2012).[243] Copyright 2012 American Chemical Society.

Next to electrochemistry, the floating water bridge provides an interesting environment to study the behavior of water in strong fields. As shown in Fig. 17, this water bridge is usually formed between two glass beakers, each containing an electrode of opposite polarity. Applying DC or AC high voltage between the electrodes leads to the formation of the bridge, which is sustained as long as the voltage is present, with the water level in the two beakers remaining unaltered. Interestingly, the internal flows in the bridge display similar behavior to Birkeland currents in gaseous plasma, with a cylindrical inner core and a tubular outer shell flowing in helical direction.[256] While the history of this experiment dates back to the end of the nineteenth century, the exact cause of its sustainability continues to be a topic of debate. However, both an analytical model and a simulation study have independently demonstrated bridge stabilization by orientational reordering of the water molecules with their dipole moments parallel to the field, resulting in chains of aligned molecular dipole moments.[257,258] The alignment is counteracted with addition of salt, in agreement with experiments.[258] The difference between the microscopic structure of the floating bridge and the one of bulk water has also been shown in other studies. In a HDO:D_2O water bridge, for instance, the lifetime of the local OH stretch vibration of HDO molecules was found to be shorter than in the bulk, while its delocalization by thermalized relaxation lasted longer.[259] The core of the bridge contains water with H^+ ions and ice-like features, while the outer shell contains more OH^- ions.[260] In the bridge, a higher H^+ mobility than in bulk water has been measured, explained with a stronger hydrogen bond and therefore stronger intermolecular proton delocalization.[261] These delocalized protons seem to result in a separation of charge, with excess charge of opposite sign in each of the beakers.[262] Superfluid properties have been attributed to the floating water bridge, based on calculation of the tension in the bridge in terms of the Maxwell pressure tensor.[257] One study suggests the formation of molecular hydrogen in the liquid, which is subsequently degassed at the surface of the bridge.[263] Remarkably, according to two other studies, a network of nano- and microbubbles might be present in the outer layer of the bridge, counteracting the surface tension and responsible for the observed light scattering, heating and strong density changes.[264,265]

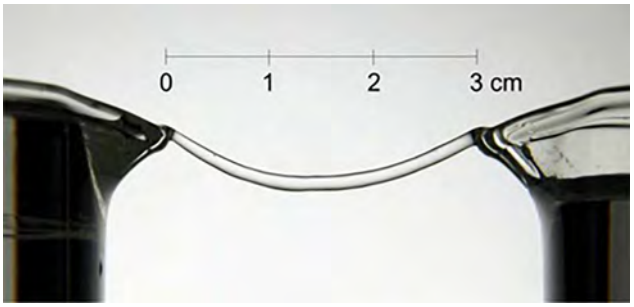

FIG. 17. A thin floating water bridge between two glass beakers for an applied DC voltage of 33 kV. Reprinted with permission from E. C. Fuchs *et al.*, Eur. Phys. J. Spec. Top. **223**(5), 959–977 (2014).[266] Copyright 2013 EDP Sciences, Springer-Verlag.

Many of these insights can be used to interpret studies on plasma initiation in water, especially for the slow mechanisms, such as the bubble and subsonic mechanism. Moreover, since the above studies correspond to the steady-state behavior of water subjected to a strong electric field without plasma formation, they also reveal the changes in microstructure that can be expected during faster plasma processes in water, such as the electronic and supersonic mechanism. We believe that studies on the transient initiating processes in surface electrochemistry and the floating water bridge can simultaneously provide more direct information for the early stages of plasma initiation. Such studies are, however, scarce (see Refs. 82 and 83 for two examples). Therefore, interdisciplinary investigation of these transient phenomena will be beneficial for all involved fields.

III. PLASMA-LIQUID INTERACTION: ELECTRICAL PROPERTIES OF THE LIQUID SURFACE

A. Electrical coupling of the worlds above and beneath: A not-so-superficial surface

Plasma is more than just the sum of its constituents. When studying gas discharges, one needs to consider the whole package. The long-range Coulomb interactions between the charged and dipolar plasma constituents bring about a collective behavior of the entire particle system. In fact, this collective behavior is exactly what differentiates gaseous plasma from neutral gas.[267] Most plasmas are quasi-neutral, meaning that the macroscopic net charge equals zero. Due to the higher mobility of free electrons as compared to heavy ions, a disturbance in the plasma, such as the addition or removal of charge, gives rise to oscillations of the electron gas relative to the ionic cores. Such plasma oscillations form the elemental manifestation of the collective behavior, characterized by the plasma frequency.[267] In weakly or partially ionized plasma, neutral-charge interactions typically dominate charge-charge interactions, resulting in a restricted and less pronounced collective behavior. Nonetheless, this behavior is still present. A special case is seen in plasma jets, where flowing inert gas at atmospheric pressure is first ionized and subsequently vented through a tube into ambient air. At the tube outlet, a plume-shaped plasma is visible by the naked eye. When observed by rapid imaging techniques, this plume can be recorded as a bullet-shaped plasma that repetitively propagates with a velocity in the order of 10 km s^{-1} or more, much faster than the gas flow.[268] This appearance accordingly was given the name "plasma bullet." As suggested by Ye and Zheng in Ref. 269, the term "bullet" is a misnomer, since it seems to imply an autonomous plasma disconnected from its region of origin. The bright bullet, namely, leaves a less-luminous yet conducting tail behind. Placing two or more plasma jets parallel and close to each other reveals another remarkable feature: the plasma plumes couple together into one amplified jet.[270] Clearly, when considering plasma, one needs to stay aware of all surroundings.

In plasma physics of liquids, this holistic view on gas discharges becomes even more important. Figure 18 shows the influence of a pulsed inhomogeneous electric field below

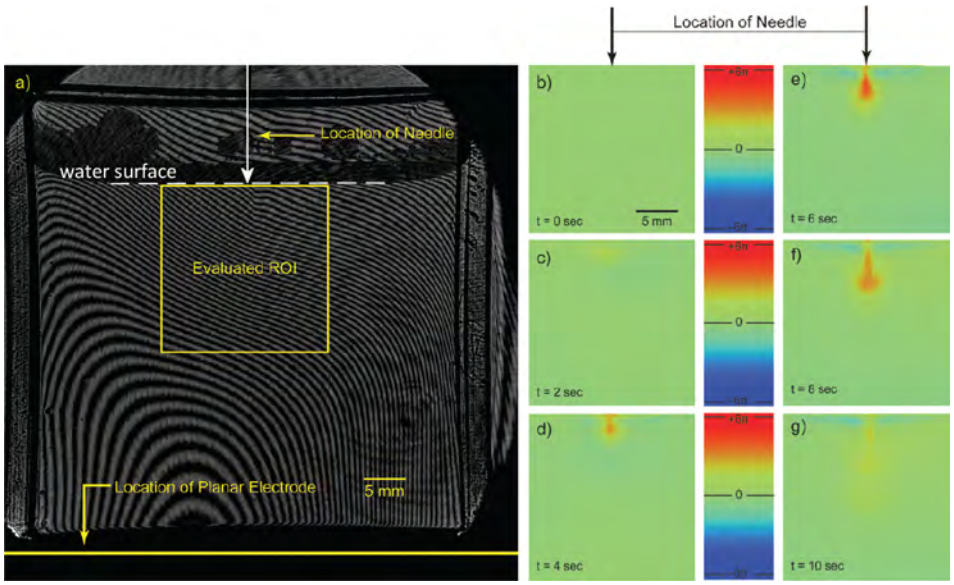

FIG. 18. (a) Interferogram of a water filled cuvet in the absence of an electric field. A downwards pointing needle electrode is located with its tip right below the water surface. The planar electrode underneath the cuvet is grounded. ROI stands for the region of interest, considered in the time evolution panels (b)-(g), which are determined from the evaluated interferograms during application of a voltage step with an amplitude of 20 kV and a rise time less than 500 ms. A positive phase shift up to 6π (red) corresponds to high refractive index and density, as in the jet, and vice versa for a negative phase shift down to -6π (blue), as in the band right underneath the liquid surface. Adapted with permission from A. D. Wexler *et al.*, Phys. Chem. Chem. Phys. **18**(24), 16281–16292 (2016). Copyright 2016 PCCP Owner Societies.

the plasma formation threshold on a volume of water, as studied in Ref. 82. A high voltage pulse is applied on a downwards oriented needle electrode, of which the tip is submerged just below the water surface. Under influence of the induced field, the fringes in the initial interferogram [Fig. 18(a)] were strongly bent in the top few millimeters of the liquid (not shown), with perturbations deep into the bulk, indicating that polarization took place over the entire liquid volume. The recorded interferograms were processed to give the time evolution panels in Figs. 18(b)–18(g), representing the space-resolved change in refractive index as well as medium density. The panels not only display a jet (red area in the pictures) moving downwards from the pin electrode, but also reveal an unanticipated band of lower density [blue feature in Fig. 18(f)] near the water surface. Electric fields can thus influence liquids over their entire volume, with strong effects on places, such as the water surface, where we would not expect them in first instance.

Similar phenomena can be expected when plasma is generated above a liquid surface. Indeed, the effect of a water surface on gas discharge behavior has been observed in a few recent studies. Vanraes *et al.* discovered unusual plasma phenomena, for instance, in a dielectric barrier discharge over a water film (see Fig. 19).[271] As can be understood from its name, this type of discharge is generated by placing one or more dielectric barriers between the electrodes, which prevents high currents and thus arc formation. Next to plasma jets, a dielectric barrier discharge over a water electrode is one of the two main plasma reactor types considered for application in plasma medicine and water treatment.[17,19,272] In the study of Vanraes *et al.*, the barrier was located on the high voltage electrode and the liquid film served as grounded electrode. For AC powered plasma, dissimilar behavior was observed by means of high speed imaging during the positive and negative voltage half cycles. When the water acted as anode [Fig. 19(a)], a short intense plasma filament appeared, comparable with the case of a dielectric barrier discharge between solid electrodes. For a water cathode [Fig. 19(b)], however, the electrical discharge lasted longer with lower intensity and a glow-like ionization wave onto the dielectric barrier was seen. Based on two other studies,[273,274] the ionization wave seemed to be characteristic for a resistive barrier discharge, an uncommon type of plasma with more diffuse features as compared to the usual dielectric barrier discharge. Moreover, a bright plasma spot was continuously witnessed near the water surface. To the best of our knowledge, this unique property has never been reported for dielectric barrier discharges with solid electrodes.

The fundamental study of plasma jets over a water surface, on the other hand, has received increasing interest in recent years. Also for this reactor configuration, the influence of the liquid surface is apparent. Three different plasma jets over a water sample were investigated in Ref. 275 and compared for the situations with and without water. For the case with water, the plasma bullets had higher velocity, intensity and gas temperature. Next to that, higher power dissipation was measured at the moment when the bullet hit the water surface. The plasma bullet impact area on the water surface was found to decrease with increasing liquid conductivity in Ref. 276. As another influence of increasing conductivity, a higher water vapor uptake into the plasma plume was detected in Ref. 277. Remarkably, the latter study reported an upwards deflected plasma bullet after impact on the liquid target. In Ref. 278, on the other hand, a change in plasma mechanism was observed when the bullet reached the water surface, which was attributed to the presence of water vapor.

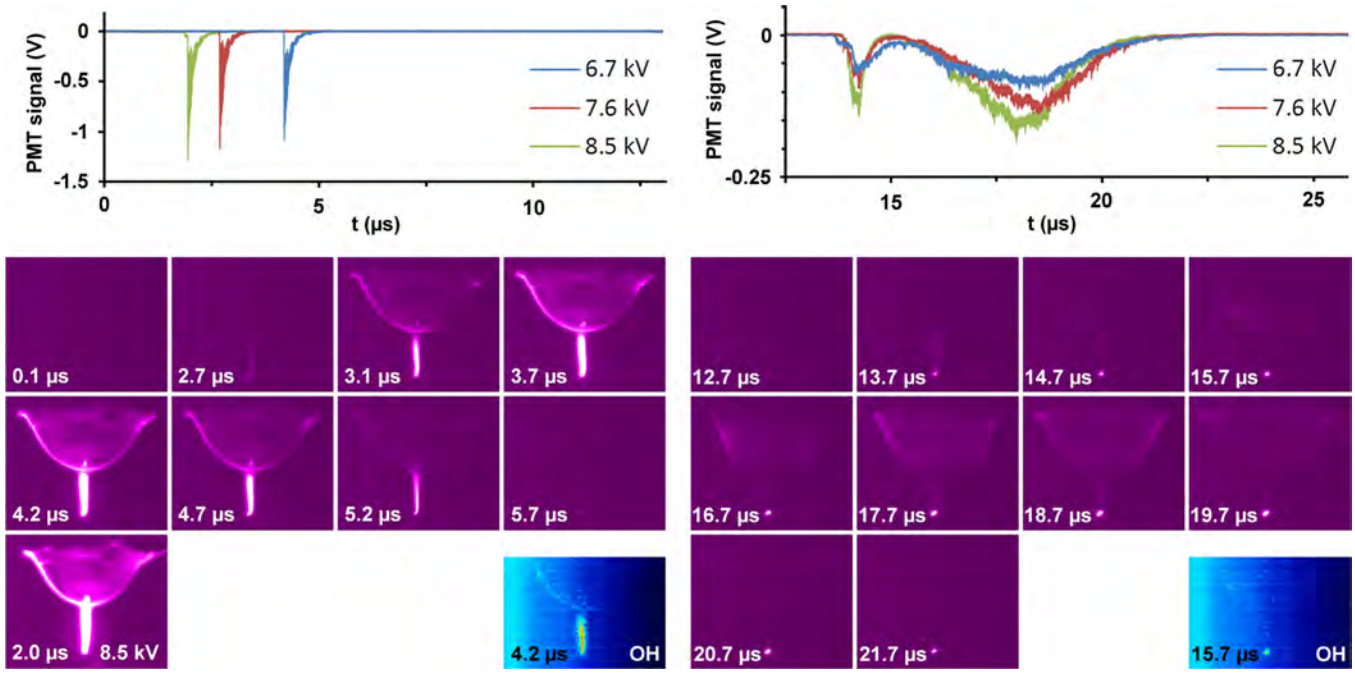

FIG. 19. Temporal behavior of an AC powered single dielectric barrier discharge filament between an upper high voltage needle included in a spherical quartz barrier and a thin water film over a grounded grid, with (top panels) the accumulated light signal from a photomultiplier tube and (bottom panels) time-resolved imaging, (left) during the negative and (right) positive voltage half cycle. The blue panels present images obtained with an OH filter. For all panels, the applied voltage amplitude was 6.7 kV, except for the most left bottom panel, where the discharge for 8.5 kV is shown for comparison. Adapted under the Creative Commons license with permission from P. Vanraes *et al*., Sci. Rep. **8**, 10919 (2018).

As seen in Fig. 20, the ring-shaped plasma bullet made a transition into a pin-like feature upon impact. Afterwards, the discharge remained present at the surface for an unusually long time. Also in this case, the bullet velocity was found to be higher than in the absence of water.

For gas discharges over a liquid surface, evaluation of the bulk liquid has mainly been performed in terms of chemistry, convection, and diffusion up to now.[40,56] To investigate other features of the liquid, diagnostic methods and simulation techniques applied in electrochemistry and in research on the floating water bridge (see Sec. II E) can be considered. Special interest goes to plasma jets and dielectric barrier discharges over a liquid surface, as these types of plasma reactors are versatile and promising for various applications, such as water treatment and plasma medicine (see the Introduction). While the number of investigations on the gaseous phase is increasing for plasma jets, the fundamental features of dielectric barrier discharge over a liquid surface are still largely left unexplored. Therefore, we promote the necessity for further and deeper investigations on these topics. In Secs. III B–III D, we will shift our focus to elemental processes at the plasma-liquid interface. As depicted in Fig. 21, surface deformation and ionic desorption will be discussed in Sec. III B, followed by electron emission mechanisms in Sec. III C. Finally, Sec. III D will shortly consider the area right above the surface.

B. Surface ion release: Surfing on capillary waves and Taylor cones

While bulk liquid displays complex microscopic behavior (see, e.g., Sec. II E for the case of water), the gas-liquid interface is considered even more complicated.[279] On the atomic scale, a liquid surface is not planar, but characterized by thermally activated capillary waves,[280] as well as perturbations induced by adsorbed surface-active solute ions.[281–283] As stated by a simulation study in Ref. 284, the molecular orientation in the interface layer depends on local surface fluctuations, since dipoles point towards the gas phase on extrusions and lie flat on the surface elsewhere. Another complexity involves the interface thickness, often defined as the distance perpendicular to the surface over which the density profile passes through 10% and 90% of the total change between bulk gas and bulk liquid.[285] This thickness strongly depends on experimental conditions, as it grows with temperature[286–288] and shrinks with surface tension.[289] According to simple theory, all salts undergo a clear interfacial charge separation with the formation of an ionic double layer, while several molecular dynamics simulations have shown this to be incorrect in some cases.[290] For the case of aqueous solutions, the exact composition and electrical structure of the interfacial region depend on the nature and bulk concentration of solutes in a complex manner. As a general trend, however, the water surface prefers to adsorb easily polarizable, large anions, whereas cations and weakly polarizable, small anions are repelled towards the liquid bulk.[290,291] Hydronium cations are remarkable exceptions, with a clear tendency towards the surface.[291] As further discussed in Sec. III C, also solvated electrons can temporarily reside near the gas phase.[157,291–293] Accordingly, it seems justified, in general, to model the upper edge of the air-water interface as a Stern layer, in analogy to the double layer theory for solid-liquid interaction. Yet, more detailed research is required to elucidate the solvation structure of specific

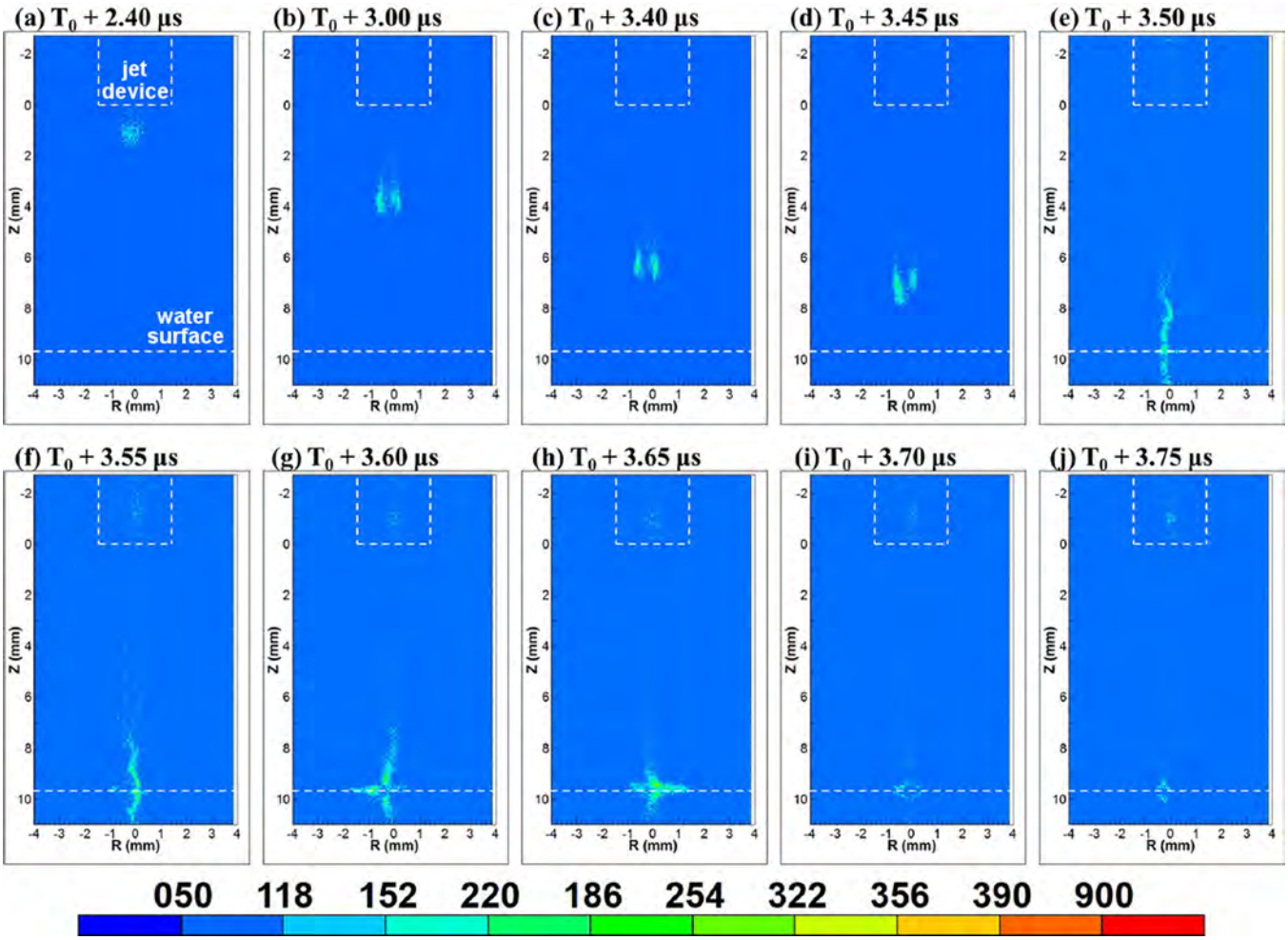

FIG. 20. High speed imaging of a propagating plasma bullet from a helium plasma jet. The time index of the images is given at the top of each frame, while the intensity legend is given in arbitrary units at the bottom of the figure. Reprinted with permission from S.-Y. Yoon *et al.*, Phys. Plasmas **24**(1), 013513 (2017). Copyright 2017 AIP Publishing LLC.

ions at the liquid surface, i.e., whether they can break out of their solvation shell and to which degree they are exposed to the gas phase. Regarding the water molecule arrangement, empirical polarizable models with fixed charge seem sufficient to estimate the oxygen-oxygen and hydrogen-oxygen radial distribution functions, hydrogen bond populations and orientational relaxation times in the interface region. Nonetheless, *ab initio* simulation is required to obtain the

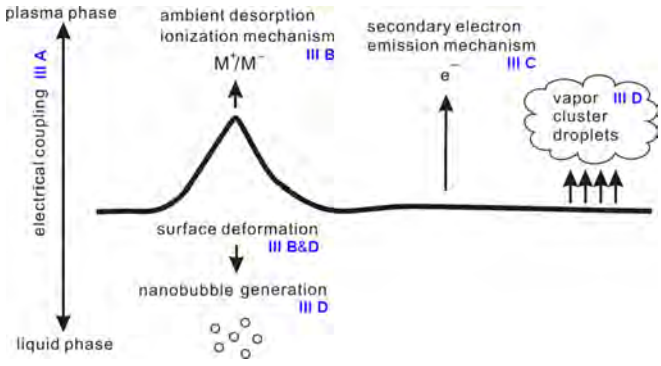

FIG. 21. Schematic overview of Sec. III. The blue codes refer to the corresponding subsection numbering. M^+/M^- stands for either a positive or negative ion.

experimentally observed drop in molecular dipole moment and the expansion in oxygen-oxygen distance near the gas phase.[294] To date, our understanding of the interfacial ion distribution, molecular orientation and surface potential in terms of the electric field is incomplete.[290] As main consensus between studies, the chemical composition at the interface shows clear differences in comparison to the bulk and simple rules seem difficult to state.[279]

Still, a liquid-plasma interface contains an even higher level of complexity, due to the external electric field, particle bombardment, space charge effects, incident radiation, locally enhanced evaporation, chemical and electrochemical processes, and so on. Several of these influences have been extensively discussed in the recent review of Bruggeman *et al.*[40] In what follows, we will shortly introduce a few other aspects that deserve, in our opinion, particular attention.

Figure 22 shows the evolution of a water surface subjected to a strong electric field, as calculated with molecular dynamics simulation.[258] First, the applied field reorders the dipolar orientation of the water molecules until a protrusion arises at the surface, which grows into a Taylor cone-like structure [Fig. 22(b)]. Depending on the exact conditions, the Taylor cone can further grow into a vertical water bridge, as depicted in Fig. 22(c) (see also Sec. II E). Before the

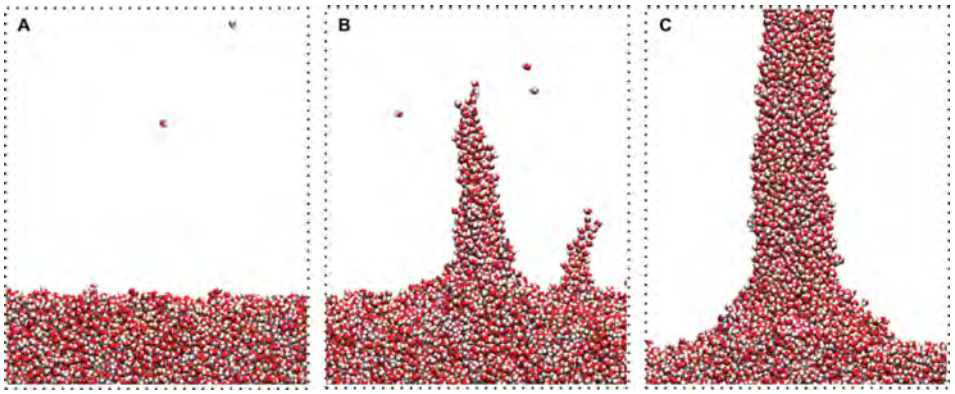

FIG. 22. A sequence of snapshots of a molecular dynamics simulation showing the water surface deformation under influence of an applied electric field (upward direction) of 2×10^9 V/m: (a) the system in the absence of the field, (b) the system in the presence of the field during a transient stage where a cone emerges from the surface, and (c) the final steady-state when the cone has grown to a cylindrical structure (so-called vertical water bridge). Red and white spheres represent oxygen and hydrogen, respectively. Reprinted with permission from J. Jirsák *et al.*, Mol. Phys. **113**(8), 848–853 (2014). Copyright 2015 Taylor & Francis Ltd. (http://www.tandfonline.com).

Taylor cone tip reaches the upper electrode, electrical breakdown can take place between the electrode and the water tip, as observed in Refs. 295 and 296. An example is shown in Fig. 23, where an oscillatory motion between formation and destruction of the bridge occurs in the presence of a high circuit resistance. As another possibility, the very strong local electric field at the tip of the cone can lead to the ejection of highly charged droplets under influence of Coulomb repulsion.[297] The charged droplets decrease in size through a combination of evaporation and fission processes, finally resulting in the formation of gas phase ions, which forms the basic mechanism of electrospray ionization.[297] Here, we enter the field of analytical chemistry, with ambient desorption ionization in particular.[298–302] Ambient desorption ionization can be understood as an umbrella term for desorption of ions from solid or liquid samples at ambient conditions. Electrospray ionization stands as but one example from a wide spectrum of methods used for this application, next to laser desorption,[303] thermal desorption,[304] and plasma-based techniques.[305–309] While it is beyond the scope of the present review to give a concise overview, we want to emphasize its relevance and importance in the fundamental mechanisms of plasma-liquid interaction. In line with Sec. III A, desorbed ions cannot only influence the local processes at the plasma-liquid interface, but might also change the overall plasma behavior. Nonetheless, many studies neglect their role, since experts in the field tend to focus mostly on the effects of plasma on the liquid (see, e.g., Refs. 40 and 56). This tendency can be explained with the main applications that drive this line of research, including water treatment and plasma medicine, where the liquid (bio)chemistry forms the main objective. We therefore aim to motivate experts from plasma physics of liquids and analytical chemistry to team up, in order to scrutinize the fundamental aspects of ambient desorption ionization, as this will strongly benefit both fields. For more information on this topic, we refer to a number of excellent reviews.[298–303,305–309]

C. Surface electron release: To be or not to be solvated, that is the question

When plasma is generated in contact with a solid surface, the properties of this surface will clearly play an important role. One of the most decisive material features in this context involves the ability of the surface to emit electrons. Electrons can be emitted as an effect of several processes, including heating of the surface, the photoelectric effect, as well as bombardment by ions, metastables and ground-state gas species with sufficient kinetic energy. Depending on the exact experimental conditions, one of these mechanisms might be dominant, permitting simplifications. For instance, one can consider the average number of emitted electrons per incident ion and give it a fancy name. In this manner, the secondary electron emission coefficient γ was born.[310] This old approach is still commonly used, especially for glow and dielectric barrier discharge.[311–313] As such, secondary electron emission coefficients are nowadays available in literature for various metals and dielectrics.[314–316] Nonetheless, one should stay aware of the simplification being made,

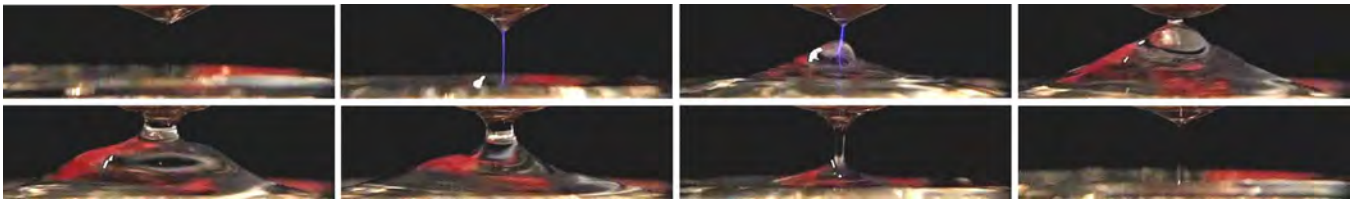

FIG. 23. Consecutive photographs (from left to right) displaying one period from an oscillatory behavior in a vertical water bridge. Initially, a filamentary plasma channel is formed in between the water surface and the upper DC electrode. Next, the water surface rises until it touches the electrode, creating a vertical water bridge. Afterwards, the surface lowers, the bridge breaks and the cycle is repeated. The time interval between the consecutive frames is 20 μs. Reproduced with permission from R. M. Namin and Z. Karimi, "Dynamics of a vertical water bridge," preprint arXiv:1309.2222 (2013).

since it might not be valid in certain cases. In the case of a dirty cathode, for example, bombardment by neutral species was found to be roughly equivalent to ion-induced electron emission in Ref. 310. Moreover, a higher kinetic energy of incident particles results in a higher secondary electron yield, making the considered coefficients a function of this energy.[310]

Today, modeling of plasma in contact with liquids is facing a crucial challenge: developing a trustworthy description for electron emission from liquid electrodes. For aqueous solutions, the ion-induced secondary electron emission coefficient can be found in a few reports for the case of glow discharge electrolysis.[57,317–320] In the review,[57] for instance, Bruggeman *et al.* mention a value range around $\gamma \approx 10^{-3} - 10^{-4}$, which is 2 to 3 orders of magnitude smaller than for metal electrodes. These values are calculated from the cathode potential drop, by applying the standard model of glow discharge between metal electrodes. Applying this model is reasonable, in the sense that a glow discharge with a water cathode displays a similar structure to the one between metal electrodes (see, e.g., Refs. 321 and 322). One should stay aware that, however, the retrieved values must be understood as indirectly measured "apparent" secondary emission coefficients, as they refer to neither a physical, nor an established material surface constant. Indeed, different authors have observed a filamentary, inhomogeneous cathode layer structure instead of a diffuse one,[321,323,324] rendering the glow discharge model *a posteriori* invalid. The plasma sustainment mechanism at a liquid cathode is therefore expected to be different from the ion-induced electron emission from metal cathodes, as mentioned in Ref. 40. According to the tunneling mechanism of Cserfalvi and Mezei, ion-induced secondary electron emission at a water cathode in glow discharge electrolysis consists of four steps:[317]

- First, bombardment of the water cathode surface with an incoming positive ion results in a solvated electron.
- Next, this electron reacts with a hydronium cation to form a neutral H atom.
- Then, the H atom diffuses through the water interface towards the gas phase.
- Finally, in the cathode dark space, the H atom is ionized, resulting in a secondary free electron.

Nonetheless, the large number of steps, as well as the slow diffusion step, makes this model questionable. Moreover, this mechanism is largely based on the observation that the calculated secondary electron emission coefficient is pH dependent for pH < 2.5, while the contribution of the corresponding change in water conductivity is not taken into account. Also, it is limited to aqueous solutions and cannot explain electron emission for other liquids, such as for ionic liquids at low pressure.[325] Gaisin and Son postulated a more universal, qualitative mechanism for secondary electron emission, where electrons are released by negative ions in the vicinity of or on the liquid cathode surface.[318] This model is based on the idea that it generally requires less energy to emit an electron from a negative ion than from ionization of H_2O, but this idea can be extended to other liquids as well.

As can be deduced from these mechanisms, there seems to be a general belief among plasma scientists that ion-induced electron emission at a water cathode is fundamentally different in nature from the mechanism known for solid metal electrodes. We want to bring to mind that this cannot be known with certainty. Namely, the deviation of a glow discharge at an aqueous cathode from the case with a metal cathode might originate from the characteristic way in which the aqueous solution compensates for the accumulated surface charge stemming from the incoming ions and extracted electrons, rather than from the emission mechanism. The charge compensation mechanism depends on electronic properties of the liquid bulk and interface, such as their distributed resistivity, capacitance, and dielectric constant. Although it possibly involves highly mobile aqueous protons (see Sec. II E and Refs. 326 and 327) as an effect of the strong field induced by the surface charge, the compensating processes will be slower than at a metal cathode.

Electron emission from a water cathode induced by a single incident ion, on the other hand, can occur on small time scales, where the liquid appears frozen in time. Therefore, the mechanism of ion-induced electron emission at a water cathode might be similar as for a solid surface, making it possible to apply a solid insulator or amorphous semiconductor model (see Sec. II B). The fundamental mechanisms of electron emission from solid insulators are very similar to the ones from solid metals.[316] Figure 24, for instance, presents potential electron emission from an insulator by an incident multi-charged ion. As the ion approaches the surface, surface electrons get captured in the empty outer shells of the ion, resulting in a so-called hollow atom, i.e., a multiply excited atom. The hollow atom, being a transient state, ejects the captured loosely bound outer-shell electrons, resulting in secondary electron emission. This mechanism can be formulated for metals, where conduction electrons are emitted, or for semiconductors and insulators, where electrons from the valence band take part in the process.[316] Slow singly charged ions can contribute as well to the potential emission mechanism, though less efficiently. Next to that, fast incident ions can transfer their energy to electrons through a kinetic emission mechanism.[328,329]

Potential and kinetic emission plausibly also occur over a liquid surface, in clear analogy. Contrary to what is intuitively expected, insulators exhibit more efficient ion-induced electron emission than metals,[316] so it is tempting to expect this for dielectric liquids with a large band gap as well. However, the compensation mechanisms for the accumulated surface charge are likely different for dielectric liquids and solids. Also, one needs to consider the distinct features of a liquid surface as compared to solids, such as the ionic double layer and types of adsorbed anions. That is, electrons from negative ions at the gas-liquid interface (see Sec. III B) might be preferable candidates for electron emission. In addition, solvated electrons might play a major role in this story. The nature of solvated electrons at the liquid surface is still controversial, with contradicting results between studies.[157,292,293,330] While in some studies, no excess electrons are detected at the surface,[330] other reports mention them with conflicting data on their stability and solvation structure.[157,292,293] According to

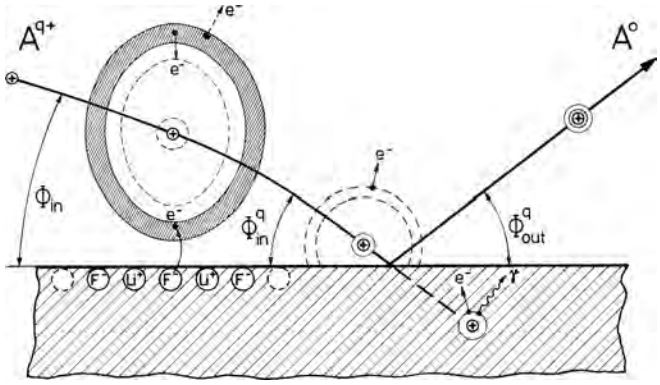

FIG. 24. Mechanism of secondary electron emission from an insulator surface (LiF salt) by an incident multi-charged ion A^{q+}. As the ion approaches the interface, the electronic potential barrier between ion and solid is gradually lowered, until surface electrons are transferred to the Rydberg levels of the ion. Electron capture and subsequent loss lead to emission of free electrons. The electron emission sequences end when the ion reaches close enough to the surface to have its inner shells filled, resulting in the formation of a neutralized species A^0. Reprinted with permission from H. Winter, Prog. Surf. Sci. **63**(7), 177–247 (2000). Copyright 2000 Elsevier.

the experiments in Ref. 293, surface electrons are completely surrounded by a solvation shell, with a lifetime exceeding 750 ps. A second study found a stable surface-bound state that was prevented from complete solvation for over 100 ps, attributed to a free-energy barrier between the gas phase and bulk liquid.[157] Surface electrons with a partial solvation shell were also reported in a more recent investigation, yet with a shorter lifetime.[292] Note in this regard that the stability and structure of surface electrons might be significantly altered in the presence of an external electric field, in analogy with the thought experiment of Fig. 8. Additionally, the prevalent reactive species at a plasma-liquid interface further complicate their stability, as discussed in Ref. 331. The latter argument, however, is not unique to plasma-liquid interaction, since, in general, solvated electrons are simultaneously formed with reactive species.

Thus, to be or not to be solvated, that is the question. Very interesting on this subject is the old model of Parilis and Kishinevskii, which explains kinetic secondary electron emission from a surface by ion bombardment with the transition from valence band electrons to the conduction band.[329] Subsequently, recombination of an electron-hole pair over the band gap occurs, where the recombination energy is transferred to a conduction band electron, resulting in the emitted electron. This model was originally formulated with an internal Auger process, but can be extended with two analogue mechanisms, which have been discovered recently for water.[332–335] In view of the "frozen liquid" model for liquid water on small time scales, Fig. 25 shows experimental values of the secondary electron emission coefficient γ for pure H_2O ice upon ion impact, taken from Ref. 336. Ice emits electrons remarkably more effective than aluminum, in agreement with the generally higher efficiency of insulators as compared to metals[316] and in line with an old qualitative report on corona discharge from ice peaks.[337] Values of γ for incident ion energy below 5 keV are, unfortunately, not found in literature. Nevertheless, these results strengthen the hypothesis that electron emission from a liquid water cathode is limited predominantly by its flowing nature and thus its charge compensation mechanism, rather than its molecular composition.

It should be emphasized that ion-induced electron emission is but one of several possible mechanisms. Thermionic emission from liquids at ambient conditions is unlikely due to the high temperatures required for this process.[57] Field-induced emission, on the other hand, requires a locally strong electric field at the surface. This process should especially be considered, as the electric field can be enhanced by surface deformation (Sec. III B) and droplets at the interface (Sec. III D). Also, ion bombardment and the electric field can combine to synergetic ion-enhanced field emission.[339] Photoemission under influence of plasma generated photons and explosive electron emission, as mentioned in Sec. II D, should also be considered at a liquid cathode. The latter two processes can, in contrast to ion-induced emission, account for electron emission in nanosecond time scales.[340] To our knowledge, explosive electron emission has up to now only been studied for solid and liquid metal surfaces, but not from a dielectric liquid.

D. Electrical properties of surface vapor: Into the mysteries of the mist

If plasma physics of liquids were a water amusement park, it surely would have a lot of attractions. In the previous sections, we have considered, among others, sub-aquatic

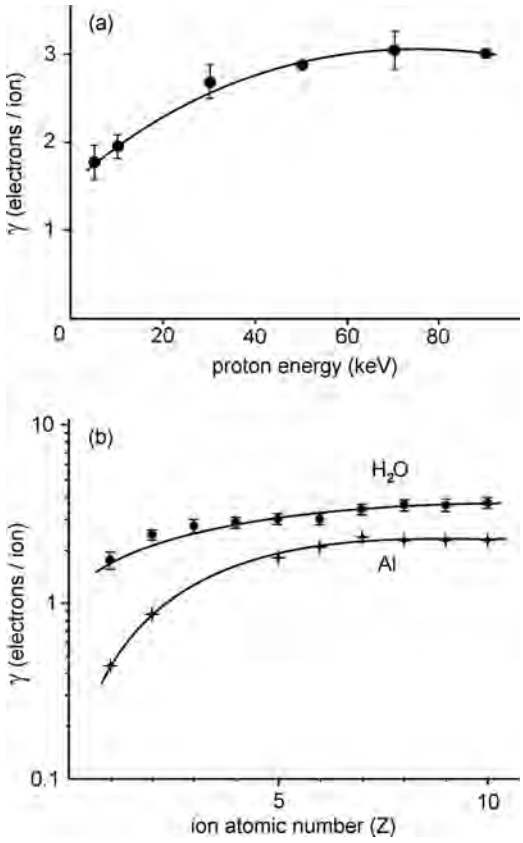

FIG. 25. Measured values of the secondary electron emission coefficient γ of an amorphous H_2O ice film (a) as a function of incident proton kinetic energy and (b) as a function of the atomic number of the incident ion at a fixed kinetic energy of 5 keV/amu, with comparison to aluminum. The graphs are based on data from Refs. 336 and 338.

activities involving underwater photography (Sec. II), the synchronized swimming of dipolar water molecules (Sec. II E), capillary wave riding by surface ions (Sec. III B), and the eruption of spraying Taylor cones as miniscule splash fountains (Sec. III B). In this section, the steam saunas and thermal pools are presented, before we revisit the nanobubble bath from Sec. II C. While these themes might look deceivingly relaxing, the conditions at the plasma-liquid interface are likely turbulent and in strong non-equilibrium. At the atomic scale, the interface is prone to various violent processes and influences, such as a continuous bombardment with ions, electrons, neutral species and photons, strong inhomogeneous fields, gaseous and liquid convection, strong density gradient driven diffusion, and different chemical reactions, including ionization, photochemistry, and electrochemistry. Some examples have been discussed in Secs. III A, III B, and III C. Others can be found in Ref. 40. Most of these processes contribute to heating of the interface and mass transfer towards the gas phase.[40] Gaseous convection and diffusion, as well as ionic drift processes under influence of the electric field, can spread the transferred mass over the entire plasma volume. Next to desorbed ions, as discussed in Sec. III B, mass is also relocated from the liquid into the gas phase in the form of solvent vapor and droplets.

Whereas a vapor layer is naturally present at a liquid surface, the properties of interfacial mist under plasma conditions are strongly influenced by the above-mentioned processes. As suggested in Ref. 321, a water surface in contact with plasma in ambient air can act as a heat sink. This locally stabilizes the discharge, in addition to electrical stabilization caused by the distributed resistance of the liquid electrode. The enhanced evaporation and water sputtering by ion bombardment [341,342] lead to higher humidity. With humidity, also the breakdown voltage in air increases. While this effect is often ascribed to electron scavenging originating from the electronegative nature of water vapor, it has been demonstrated in Ref. 343 that electron detachment and ion conversion processes need to be taken into account as well. Although the critical breakdown field (not to be confused with the breakdown voltage) is unaltered with addition of water vapor, the humidity effect is caused by nondetaching cluster ion formation upon collisions of negative ions with H_2O molecules. For instance, H_2O molecules cluster with O_2^- through cascade reactions[344]

$$O_2^- + H_2O + M \longleftrightarrow O_2^-(H_2O) + M, \quad (1)$$

$$O_2^-(H_2O) + H_2O + M \longleftrightarrow O_2^-(H_2O)_2 + M, \quad (2)$$

$$O_2^-(H_2O)_2 + H_2O + M \longleftrightarrow O_2^-(H_2O)_3 + M, \quad (3)$$

with $M = N_2$ or O_2 and where the energy required for electron detachment increases with cluster size. In atmospheric air, $O_2^-(H_2O)_3$ is the most probable cluster.[344] This clustering behavior of water is caused by the dipolar nature of H_2O molecules. It occurs for both positive and negative ions, but is more pronounced for the negative ones.[345] Note that this complicates secondary electron emission from negative ions at the liquid cathode surface, as postulated by Gaisin and Son (see Sec. III C). When water micro- or nanodroplets are dispersed in air, on the other hand, the breakdown voltage is reduced due to an enhanced electric field in the close vicinity of the droplets,[346] similar to field enhancement in the liquid phase by nanobubbles (Sec. II B) and nanoparticles (Sec. II C). In particular, droplets can locally strengthen the electric field near the liquid surface, comparable with the strong field at a Taylor cone tip (Sec. III B). This could lead to field-assisted electron emission from the liquid electrode (Sec. III C). Microdroplets have been observed during operation of the floating water bridge by Fuchs *et al.*[347] The latter authors explained the droplet formation with field-induced electrospray processes and the break-up of microjets by capillary waves on the liquid surface (see also Sec. III B).

As should be emphasized, the liquid surface can deform in various ways under plasma contact. In clear contrast to Taylor cones (see Sec. III B), penetration of plasma into the liquid bulk volume has been reported in Refs. 348 and 349. Hoffer *et al.* observed this phenomenon in a pulsed discharge between a water electrode and a high voltage needle located 1 mm above the liquid surface.[349] The surface remained smooth when the liquid conductivity was higher than the conductivity of the adjacent plasma, but displayed instabilities in the opposite case. The instabilities consequently developed into elongated gas cavities or thin streamers (see Sec. II A), propagating into the liquid phase. The effect was attributed to enhanced liquid evaporation in surface instabilities due to a locally higher current density. A similar observation was made by Vanraes *et al.* for a pulsed discharge in a stationary bubble attached to a needle electrode in water.[348] Figure 26 shows the evolution of plasma and bubble shape during the voltage application. Initially, plasma fills the bubble with preferable location at the interface, while the bubble shape is not visibly disturbed. After 20 μs, the bubble expands and its surface blurs, indicating evaporation of the surrounding liquid. Instabilities occur 30 μs after voltage application, which grow into streamers at later times.

These observations imply that micro- and nanobubbles might be produced in the bulk liquid during plasma-liquid interaction. Actually, many of the above-mentioned plasma-induced interfacial processes, such as ion bombardment, irradiation, convection, and chemistry, can contribute to nanobubble formation near the liquid surface. Plasmas in contact with a water anode or cathode, for instance, generate aqueous H_2 and O_2 at the interface, respectively.[55] In sufficiently high concentration, these dissolved gases will accumulate as a separate phase in the form of nanobubbles. This expectation is supported by an increasing number of reports on the production of hydrogen and oxygen bulk nanobubbles by similar electrochemical mechanisms at submerged solid electrodes.[191,199,350–352] Next to that, dissolved gaseous compounds can also result from the interaction of the liquid with plasma produced photons. In this regard, the photon energy will be important. Long wavelength UV radiation easily passes through the water bulk, leading to a relatively low degree of photolytic chemistry. Vacuum ultraviolet radiation, on the other hand, is effectively scavenged by the first 0.1–10 μm layer of liquid, depending on the specific wavelength and the liquid composition.[40,353] More specifically, pure water has a cutoff frequency around 180 nm, which

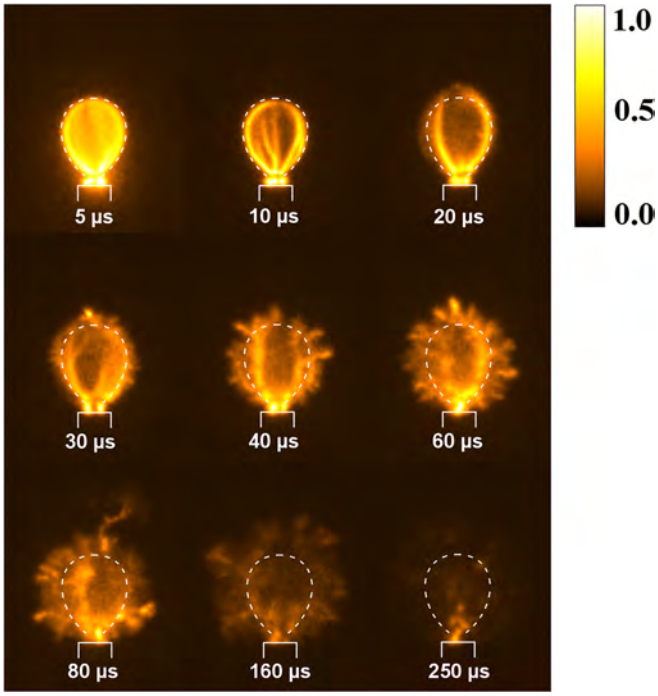

FIG. 26. Snapshots of pulsed plasma evolution in a 100 μl air bubble on a high voltage needle electrode in water, showing plasma penetration (streamers) into the liquid bulk. The continuous white line depicts the shape and position of the needle electrode, while the white dashed line represents the initial bubble contour. The time after voltage pulse application is given in every image and the color legend indicates the range from low (0.0) to high (1.0) relative intensity. Reproduced with permission from P. Vanraes, A. Nikiforov, M. Lessiak, and C. Leys, J. Phys.: Conf. Ser. **406**(1), 012013 (2012).

shifts to higher values up to 230 nm for other bio-relevant liquids.[353] Photo-dissociation of water by the absorbed photons generates H radicals, which can recombine to dissolved H_2.[55] As such, hydrogen nanobubbles can presumably be formed near the liquid surface under vacuum ultraviolet radiation at sufficiently high intensity. Although electrical discharge in dry atmospheric air does not display significant light emission with wavelengths below 280 nm, plasmas in direct contact with water might deliver a substantial vacuum ultraviolet flux on the liquid surface due to the addition of water vapor, as suggested in Ref. 40. The argon plasma jet kINPen, for instance, was found to emit a continuum of vacuum ultraviolet radiation over aqueous samples, which contributed appreciably to the total amount of aqueous reactive oxygen species produced by the plasma.[353] However, this part of its emission spectrum was mainly produced by argon excimers, whereas water vapor species only provided two spectral lines. The situation for other plasma sources in contact with water, particularly in air atmosphere, therefore remains to be explored.

So far, the generation of stable nanobubble solutions under plasma treatment has not been evidenced, to the best of our knowledge. Yet, the likelihood of this hypothesis is underlined by several indications found in literature. For instance, aqueous nanobubble solutions produce hydroxyl radicals,[354,355] which makes them interesting for water treatment (see Refs. 190 and 192 for two reviews) and agricultural applications. Indeed, experimental studies have shown the growth promotion of plants, fish, and mice by nanobubbles.[354–356] Both applications are reminiscent of the observed effects induced by plasma treated solutions.[357,358] Figure 27, for instance, draws an analogy between the favorable long-term effect of plasma treated water and nanobubble solution as fertilizer on the growth of plants. Remarkably, plasma treated solutions have reported lifetimes very similar to the ones ascribed to nanobubbles (compare, e.g., Refs. 186, 359, and 360) suggesting that the biological effects of plasma treated solutions might be caused, at least partly, by nanobubbles generated during plasma treatment. This is an extremely important possibility that begs for further investigation. This is an extremely important possibility that begs for further investigation. Especially in the context of biomedical applications, such as cancer treatment, the possible role of nanobubbles should not be overlooked.

In summary, a liquid surface is generally covered by an interfacial mist, consisting of solvent vapor, clusters, micro-, and nanodroplets, which influence the plasma in different ways. Water vapor forms negative clusters which increase the breakdown voltage, while droplets locally enhance the electric field. As the interfacial plasma mist has the ability to penetrate into the liquid, nanobubbles might be produced under plasma treatment, which can have important consequences for its application.

IV. THE FUTURE OF PLASMA PHYSICS OF LIQUIDS

Through the years, plasma physics of liquids has met multiple achievements and breakthroughs, where progress in applications has been ahead of the elementary understanding of the involved processes, as in most fields of science. With the fast improvements in available diagnostic and simulation methods, the fundamental insight has grown in recent years, on topics as laser-induced excitation of liquids, the electronic and bubble initiation mechanisms of voltage-induced plasma in the liquid phase, in-liquid streamer propagation, and gas phase discharge in contact with a liquid. Next to that, this field can appeal to an abundance of available data and models on comparable plasma systems without liquids. Nonetheless, its research landscape is still marked by multiple challenges and knowledge gaps. In order to address them, the present review aims to open the borders between plasma physics of liquids and closely related domains, where interconnections are yet largely unexplored or insufficiently developed. For in-liquid plasma, we accentuated the relevance of amorphous semiconductor physics, the emerging field of nanobubble science, electrochemistry, the floating water bridge, as well as interface science, solid breakdown, and plasmonic nanobubbles in the context of the newly proposed interface mechanism. In the second half of this review, we discussed the close relationship of plasma-liquid interaction with surface science and analytical chemistry, with ambient desorption ionization, in particular.

In the light of this interdisciplinary perspective, many research opportunities have presented themselves. For in-liquid plasma, these include the investigation of the microscopic liquid structure, with solvated electrons and nanobubbles, in particular, in the presence of strong homogeneous or inhomogeneous electric fields. A research question of special

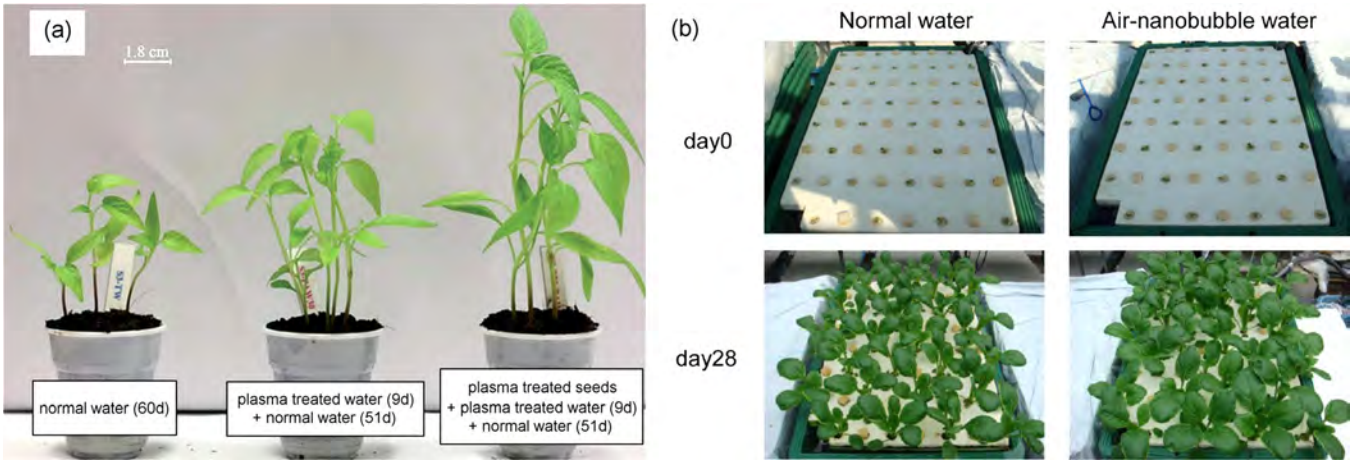

FIG. 27. (a) Effect of plasma treated water as fertilizer on the growth of pepper plants 60 days after sowing with (left) a plant given normal water, (middle) a plant given plasma treated water for the first 9 days and afterwards normal water, and (right) a plant given the same water as the plant in the middle, but the seeds were pre-treated with plasma as well. (b) Growth of 32 stumps of *Brassica campestris* cultured with (left) normal water or (right) air nanobubble solution for 4 weeks. The similarities between the biological effects of both fertilizer solutions is one of the indications (see the text) that plasma treated water might contain a high density of nanobubbles. Figure (a) is reproduced with permission from L. Sivachandiran and A. Khacef, RSC Adv. **7**(4), 1822–1832 (2017). Copyright 2017 Royal Society of Chemistry. Figure (b) is reproduced with permission from Ebina *et al.* PLoS One **8**(6), e65339 (2013). Copyright 2013 PLOS.

interest involves the prevalence of nanobubbles, nanoparticles, and their clusters in the bulk liquid and on electrode surfaces in plasma-liquid systems. Next to that, the oxide nanolayer on the submerged high voltage electrode requires to be evaluated in its thickness, shape, and electronic features. Concerning gas phase plasma in contact with a liquid, some of the main challenges comprise the assessment of ion and electron emission mechanisms, microscopic changes in the interface structure, and the possibility of nanobubble generation by means of plasma treatment.

In order to address these research questions, several strategies are available. We want to emphasize the numerous opportunities for molecular dynamics simulations in many of the mentioned topics. Next to that, classical or semiclassical models can be developed based on the available successful models from the neighboring domains, including the lucky-drift model (Fig. 5), the metal-oxide-liquid junction description of Lewis (Fig. 14), and the electron emission mechanisms for solid surfaces. As a new experimental approach, the experimental setups and diagnostic techniques from these domains, such as nanobubble science, the floating water bridge, electrochemistry, and surface and interface science, might be combined with the traditional techniques in plasma physics of liquids. We are convinced that this combined experimental and modeling strategy will enhance scientific progress, with benefits for all involved research domains.

ACKNOWLEDGMENTS

P. Vanraes acknowledges funding by a University of Antwerp BOF grant. The authors express their gratitude to Professor Dr. Peter Bruggeman (University of Minnesota, USA) for very useful comments on a draft of Sec. III C. P. Vanraes is very grateful to Professor Dr. Lars Pettersson (Stockholm University, Sweden) for the interesting discussions on the microscopic structure of water, to Dr. Xiaolong Deng (National University of Defense Technology, China) for his help with the figures, to Dr. Anton Nikiforov (Ghent University, Belgium) for the help with retrieving the relevant chapter of Ref. 319, and to Dr. Tatiana Nikitenko (Vitebst State Masherov University, Belarus), Katja Nygard (Netherlands), Iryna Kuchakova (Ghent University, Belgium), and Mindaugas Keršys (Lithuania) for their tremendous help with the translation of the corresponding chapter.

[1]J. Kuffel and P. Kuffel, *High Voltage Engineering Fundamentals* (Newnes, 2000).
[2]S. Kumar, R. Singh, T. Singh, and B. Sethi, J. Mater. Process. Technol. **209**(8), 3675–3687 (2009).
[3]Q. He, Z. Zhu, and S. Hu, Appl. Spectrosc. Rev. **49**(3), 249–269 (2014).
[4]M. Smoluch, P. Mielczarek, and J. Silberring, Mass Spectrom. Rev. **35**(1), 22–34 (2016).
[5]S. K. Pankaj and K. M. Keener, Curr. Opinion Food Sci. **16**, 49–52 (2017).
[6]J. E. Foster, Phys. Plasmas **24**(5), 055501 (2017).
[7]M. Hijosa-Valsero, R. Molina, A. Montràs, M. Müller, and J. M. Bayona, Environ. Technol. Rev. **3**(1), 71–91 (2014).
[8]M. Magureanu, N. B. Mandache, and V. I. Parvulescu, Water Res. **81**, 124–136 (2015).
[9]D. V. Palanker, U.S. Patent No. 6,135,998 (2000).
[10]Q. Shi, N. Vitchuli, J. Nowak, Z. Lin, B. Guo, M. McCord, M. Bourham, and X. Zhang, J. Polym. Sci. B: Polym. Phys. **49**(2), 115–122 (2011).
[11]F. Chen, X. Huang, D-g Cheng, and X. Zhan, Int. J. Hydrogen Energy **39**(17), 9036–9046 (2014).
[12]B. R. Locke and K.-Y. Shih, Plasma Sources Sci. Technol. **20**(3), 034006 (2011).
[13]Q. Chen, J. Li, and Y. Li, J. Phys. D: Appl. Phys. **48**(42), 424005 (2015).
[14]S. Horikoshi and N. Serpone, RSC Adv. **7**(75), 47196–47218 (2017).
[15]N. Boussetta and E. Vorobiev, C. R. Chim. **17**(3), 197–203 (2014).
[16]M. Ito, T. Ohta, and M. Hori, J. Korean Phys. Soc. **60**(6), 937–943 (2012).
[17]G. Fridman, G. Friedman, A. Gutsol, A. B. Shekhter, V. N. Vasilets, and A. Fridman, Plasma Process. Polym. **5**(6), 503–533 (2008).
[18]J.-H. Kim, M.-A. Lee, G.-J. Han, and B.-H. Cho, Acta Odontol. Scand. **72**(1), 1–12 (2014).
[19]H. Tanaka, K. Ishikawa, M. Mizuno, S. Toyokuni, H. Kajiyama, F. Kikkawa, H.-R. Metelmann, and M. Hori, Rev. Mod. Plasma Phys. **1**(1), 3 (2017).

[20]P. Vanraes, A. Nikiforov, and C. Leys, in *Plasma Science and Technology: Progress in Physical States and Chemical Reactions*, edited by T. Mieno (InTech, 2016), pp. 457–506.
[21]Y. S. Akishev, V. Karalnik, M. Medvedev, A. Petryakov, N. Trushkin, and A. Shafikov, Eur. Phys. J. Appl. Phys. **79**(1), 10803 (2017).
[22]S. B. Leonov, V. Petrishchev, and I. V. Adamovich, J. Phys. D: Appl. Phys. **47**(46), 465201 (2014).
[23]P. Lukes, M. Clupek, and V. Babicky, IEEE Trans. Plasma Sci. **39**(11), 2644–2645 (2011).
[24]C. Winters, V. Petrishchev, Z. Yin, W. R. Lempert, and I. V. Adamovich, J. Phys. D: Appl. Phys. **48**(42), 424002 (2015).
[25]A. Aleksandrov, D. Vaulin, A. Ershov, and V. Chernikov, Moscow Univ. Phys. Bull. **64**(1), 100–102 (2009).
[26]S. Kanazawa, M. Hirao, M. Kocik, and J. Mizeraczyk, J. Plasma Fusion Res. Ser. **8**, 615–618 (2009), see http://www.jspf.or.jp/JPFRS/PDF/Vol8/jpfrs2009_08-0615.pdf.
[27]N. S. Midi and R.-I. Ohyama, paper presented at Annual Report Conference on the Electrical Insulation and Dielectric Phenomena (CEIDP) (2011).
[28]M. Sato, T. Tokutake, T. Ohshima, and A. T. Sugiarto, IEEE Trans. Indus. Appl. **44**(5), 1397–1402 (2008).
[29]T. H. Khalaf and A. H. Kadum, Iraqi J. Phys. **8**(11), 88–94 (2010), see https://www.iasj.net/iasj?func=fulltext&aId=5011.
[30]J. Li, W. Si, X. Yao, and Y. Li, IEEE Trans. Dielectr. Electr. Insul. **16**(6), 1640–1647 (2009).
[31]J. Jadidian, M. Zahn, N. Lavesson, O. Widlund, and K. Borg, Appl. Phys. Lett. **100**(17), 172903 (2012).
[32]P. Atten and A. Saker, IEEE Trans. Electr. Insul. **28**(2), 230–242 (1993).
[33]L. Kebbabi and A. Beroual, J. Phys. D: Appl. Phys. **39**(1), 177 (2005).
[34]M.-X. Zhu, Y. Li, Y.-H. Wei, J.-B. Deng, H.-B. Mu, and G.-J. Zhang, IEEE Trans. Dielectr. Electr. Insul. **22**(5), 2661–2668 (2015).
[35]P. J. Bruggeman and B. R. Locke, in *Low Temperature Plasma Technology—Methods and Applications*, edited by P. K. Chu and L. XinPei (CRC Press, Boca Raton, FL, 2014), pp. 367-399.
[36]B. Jiang, J. Zheng, S. Qiu, M. Wu, Q. Zhang, Z. Yan, and Q. Xue, Chem. Eng. J. **236**, 348–368 (2014).
[37]B. Locke, M. Sato, P. Sunka, M. Hoffmann, and J.-S. Chang, Ind. Eng. Chem. Res. **45**(3), 882–905 (2006).
[38]M. A. Malik, Plasma Chem. Plasma Process. **30**(1), 21–31 (2010).
[39]S. Samukawa, M. Hori, S. Rauf, K. Tachibana, P. Bruggeman, G. Kroesen, J. C. Whitehead, A. B. Murphy, A. F. Gutsol, and S. Starikovskaia, J. Phys. D: Appl. Phys. **45**(25), 253001 (2012).
[40]P. Bruggeman *et al.*, Plasma Sources Sci. Technol. **25**(5), 053002 (2016).
[41]I. Adamovich, S. Baalrud, A. Bogaerts, P. Bruggeman, M. Cappelli, V. Colombo, U. Czarnetzki, U. Ebert, J. Eden, and P. Favia, J. Phys. D: Appl. Phys. **50**(32), 323001 (2017).
[42]N. Y. Babaeva, R. Berry, G. Naidis, B. Smirnov, E. E. Son, and D. Tereshonok, High Temp. **54**(5), 745–766 (2016).
[43]H. Bluhm, *Pulsed Power Systems: Principles and Applications* (Springer-Verlag, Berlin, Heidelberg, 2006), pp. 7-54.
[44]J. E. Foster, B. Sommers, and S. Gucker, Jpn. J. Appl. Phys., Part 1 **54**(1S), 01AF05 (2015).
[45]R. P. Joshi, J. F. Kolb, S. Xiao, and K. H. Schoenbach, Plasma Process. Polym. **6**(11), 763–777 (2009).
[46]R. P. Joshi and S. M. Thagard, Plasma Chem. Plasma Process. **33**(1), 1–15 (2013).
[47]J. Kolb, R. Joshi, S. Xiao, and K. Schoenbach, J. Phys. D: Appl. Phys. **41**(23), 234007 (2008).
[48]O. Lesaint, J. Phys. D: Appl. Phys. **49**(14), 144001 (2016).
[49]B. R. Locke and S. M. Thagard, Plasma Chem. Plasma Process. **32**(5), 875–917 (2012).
[50]N. Ramli, S. Zaaba, M. Mustaffa, and A. Zakaria, AIP Conf. Proc. **1824**(1), 030015 (2017).
[51]A. Sun, C. Huo, and J. Zhuang, High Voltage **1**(2), 74–80 (2016).
[52]L. Zhu, Z.-H. He, Z.-W. Gao, F.-L. Tan, X.-G. Yue, and J.-S. Chang, J. Electrostat. **72**(1), 53–58 (2014).
[53]A. Denat, IEEE Trans. Dielectr. Electr. Insul. **13**(3), 518–525 (2006).
[54]M. N. Shneider and M. Pekker, *Liquid Dielectrics in an Inhomogeneous Pulsed Electric Field* (IOP Publishing, 2016).
[55]R. Akolkar and R. M. Sankaran, J. Vac. Sci. Technol. A **31**(5), 050811 (2013).
[56]J.-L. Brisset and J. Pawlat, Plasma Chem. Plasma Process. **36**(2), 355–381 (2016).
[57]P. Bruggeman and C. Leys, J. Phys. D: Appl. Phys. **42**(5), 053001 (2009).
[58]J. B. Whitehead, Trans. Am. Inst. Electr. Eng. **54**(12), 1288–1291 (1935).
[59]A. Starikovskiy, Y. Yang, Y. I. Cho, and A. Fridman, Plasma Sources Sci. Technol. **20**(2), 024003 (2011).
[60]M. Shneider, M. Pekker, and A. Fridman, IEEE Trans. Dielectr. Electr. Insul. **19**(5), 1579–1582 (2012).
[61]J. Hernandez-Avila, N. Bonifaci, and A. Denat, IEEE Trans. Dielectr. Electr. Insul. **1**(3), 412–418 (1994).
[62]J. Kim, S. Dardin, K. Jackson, R. Kadel, J. Kadyk, V. Peskov, and W. Wenzel, IEEE Trans. Nucl. Sci. **49**(4), 1851–1856 (2002).
[63]G. Bressi, M. Cambiaghi, G. Carugno, E. Conti, and E. D'Uscio, Nucl. Instrum. Methods Phys. Res. Sect. A **310**(3), 613–617 (1991).
[64]M. Miyajima, K. Masuda, A. Hitachi, T. Doke, T. Takahashi, S. Konno, T. Hamada, S. Kubota, A. Nakamoto, and E. Shibamura, Nucl. Instrum. Methods **134**(2), 403–405 (1976).
[65]A. Policarpo, V. Chepel, M. Lopes, V. Peskov, P. Geltenbort, R. F. Marques, H. Araújo, F. Fraga, M. Alves, and P. Fonte, Nucl. Instrum. Methods **365**(2-3), 568–571 (1995).
[66]E. Aprile, H. Contreras, L. Goetzke, A. M. Fernandez, M. Messina, J. Naganoma, G. Plante, A. Rizzo, P. Shagin, and R. Wall, J. Instrum. **9**(11), P11012 (2014).
[67]J. Proud and J. Auborn, Appl. Phys. Lett. **27**(5), 265–267 (1975).
[68]L. Dumitrescu, O. Lesaint, N. Bonifaci, A. Denat, and P. Notingher, J. Electrostat. **53**(2), 135–146 (2001).
[69]M. Haidara and A. Denat, IEEE Trans. Electr. Insul. **26**(4), 592–597 (1991).
[70]V. Atrazhev, E. Dmitriev, and I. Iakubov, IEEE Trans. Electr. Insul. **26**(4), 586–591 (1991).
[71]N. Bonifaci, A. Denat, and V. Atrazhev, J. Phys. D: Appl. Phys. **30**(19), 2717 (1997).
[72]A. Buzulutskov, J. Instrum. **7**(02), C02025 (2012).
[73]V. Chepel and H. Araújo, J. Instrum. **8**(04), R04001 (2013).
[74]L. Arazi, A. Coimbra, R. Itay, H. Landsman, L. Levinson, B. Pasmantirer, M. Rappaport, D. Vartsky, and A. Breskin, J. Instrum. **8**(12), C12004 (2013).
[75]A. Breskin, J. Phys.: Conf. Ser. **460**(1), 012020 (2013).
[76]I. Marinov, S. Starikovskaia, and A. Rousseau, J. Phys. D: Appl. Phys. **47**(22), 224017 (2014).
[77]S. M. Korobeinikov, A. V. Melekhov, and A. S. Besov, High Temp. **40**(5), 652–659 (2002).
[78]M. N. Shneider and M. Pekker, Phys. Rev. E **87**(4), 043004 (2013).
[79]Y. Seepersad, M. Pekker, M. N. Shneider, A. Fridman, and D. Dobrynin, J. Phys. D: Appl. Phys. **46**(35), 355201 (2013).
[80]Y. Seepersad, M. Pekker, M. N. Shneider, D. Dobrynin, and A. Fridman, J. Phys. D: Appl. Phys. **46**(16), 162001 (2013).
[81]M. Pekker, Y. Seepersad, M. N. Shneider, A. Fridman, and D. Dobrynin, J. Phys. D: Appl. Phys. **47**(2), 025502 (2014).
[82]A. D. Wexler, S. Drusová, J. Woisetschläger, and E. C. Fuchs, Phys. Chem. Chem. Phys. **18**(24), 16281–16292 (2016).
[83]J. Kolb, Y. Minamitani, S. Xiao, X. Lu, M. Laroussi, R. Joshi, K. Schoenbach, E. Schamiloglu, and J. Gaudet, paper presented at the Pulsed Power Conference (IEEE, 2005).
[84]Y. Seepersad, A. Fridman, and D. Dobrynin, J. Phys. D: Appl. Phys. **48**(42), 424012 (2015).
[85]V. Y. Ushakov, V. F. Klimkin, and S. M. Korobeynikov, *Impulse Breakdown of Liquids* (Springer-Verlag, Berlin, Heidelberg, 2007).
[86]P. Gournay and O. Lesaint, J. Phys. D: Appl. Phys. **27**(10), 2117 (1994).
[87]I. Lisitsyn, H. Nomlyama, S. Katsuki, and H. Akiyama, IEEE Trans. Dielectr. Electr. Insul. **6**(3), 351–356 (1999).
[88]J. Qian, R. Joshi, J. Kolb, K. Schoenbach, J. Dickens, A. Neuber, M. Butcher, M. Cevallos, H. Krompholz, and E. Schamiloglu, J. Appl. Phys. **97**(11), 113304 (2005).
[89]G. Naidis, J. Phys. D: Appl. Phys. **49**(23), 235208 (2016).
[90]N. Y. Babaeva and M. J. Kushner, IEEE Trans. Plasma Sci. **36**(4), 892–893 (2008).
[91]N. Y. Babaeva and M. J. Kushner, Plasma Sources Sci. Technol. **18**(3), 035009 (2009).
[92]X. Li, Y. Liu, G. Zhou, S. Liu, and F. Lin, J. Phys. D: Appl. Phys. **50**(25), 255301 (2017).
[93]V. Fortov, I. Iakubov, and A. Khrapak, *Physics of Strongly Coupled Plasma* (Oxford University Press, 2006).
[94]A. Piel, *Plasma Physics* (Springer, 2017), pp. 29–44.
[95]P.-M. Robitaille, Prog. Phys. **3**, 60 (2011), see http://www.ptep-online.com/complete/PiP-2011-03.pdf.

[96]S. Hamaguchi, K. Ikuse, and T. Kanazawa, paper presented at the Proceedings of the 12th Asia Pacific Physics Conference (APPC12) (2014).
[97]A. M. Lietz and M. J. Kushner, J. Phys. D: Appl. Phys. **49**(42), 425204 (2016).
[98]C. Van Gils, S. Hofmann, B. Boekema, R. Brandenburg, and P. Bruggeman, J. Phys. D: Appl. Phys. **46**(17), 175203 (2013).
[99]W. Van Boxem, J. Van der Paal, Y. Gorbanev, S. Vanuytsel, E. Smits, S. Dewilde, and A. Bogaerts, Sci. Rep. **7**(1), 16478 (2017).
[100]R. Joshi, J. Qian, G. Zhao, J. Kolb, K. Schoenbach, E. Schamiloglu, and J. Gaudet, J. Appl. Phys. **96**, 5129–5139 (2004).
[101]D. Bolmatov, V. Brazhkin, and K. Trachenko, Sci. Rep. **2**, 421 (2012).
[102]H. Ge, H. Li, S. Mei, and J. Liu, Renewable Sustainable Energy Rev. **21**, 331–346 (2013).
[103]N. Linz, S. Freidank, X.-X. Liang, H. Vogelmann, T. Trickl, and A. Vogel, Phys. Rev. B **91**(13), 134114 (2015).
[104]B. Boates and S. A. Bonev, Phys. Rev. B **83**(17), 174114 (2011).
[105]A. Mirzoev, A. Mirzoev, Jr., A. Sobolev, and B. Gelchinski, J. Phys.: Condens. Matter **20**(11), 114104 (2008).
[106]C. Desgranges and J. Delhommelle, J. Phys. Chem. B **118**(11), 3175–3182 (2014).
[107]L. Calderín, L. González, and D. González, J. Phys.: Condens. Matter **23**(37), 375105 (2011).
[108]D. Li, H. Liu, S. Zeng, C. Wang, Z. Wu, P. Zhang, and J. Yan, Sci. Rep. **4**, 5898 (2014).
[109]V. Lazic and S. Jovićević, Spectrochim. Acta B **101**, 288–311 (2014).
[110]N. Linz, S. Freidank, X.-X. Liang, and A. Vogel, Phys. Rev. B **94**(2), 024113 (2016).
[111]J. Dharmadhikari, A. Dharmadhikari, K. Kasuba, H. Bharambe, J. D'Souza, K. Rathod, and D. Mathur, Sci. Rep. **6**, 27515 (2016).
[112]C. Sacchi, JOSA B **8**(2), 337–345 (1991).
[113]S. Minardi, C. Milián, D. Majus, A. Gopal, G. Tamošauskas, A. Couairon, T. Pertsch, and A. Dubietis, Appl. Phys. Lett. **105**(22), 224104 (2014).
[114]F. Ambrosio, G. Miceli, and A. Pasquarello, J. Phys. Chem. B **120**(30), 7456–7470 (2016).
[115]W. Chen, F. Ambrosio, G. Miceli, and A. Pasquarello, Phys. Rev. Lett. **117**(18), 186401 (2016).
[116]V. R. Kumar and P. P. Kiran, Opt. Lett. **40**(12), 2802–2805 (2015).
[117]J. Noack and A. Vogel, IEEE J. Quantum Electron. **35**(8), 1156–1167 (1999).
[118]O. Samek, D. C. Beddows, J. Kaiser, S. V. Kukhlevsky, M. Liska, H. H. Telle, and J. Young, Opt. Eng. **39**(8), 2248–2262 (2000).
[119]R. Hellwarth, Prog. Quantum Electron. **5**, 1–68 (1977).
[120]J. Frenkel, *Kinetic Theory of Liquids* (Oxford University Press, 1946).
[121]V. Brazhkin and K. Trachenko, J. Non-Cryst. Solids **407**, 149–153 (2015).
[122]E. Burkel, Rep. Prog. Phys. **63**(2), 171 (2000).
[123]K. Trachenko and V. Brazhkin, Sci. Rep. **3**, 2188 (2013).
[124]K. Trachenko and V. Brazhkin, Rep. Prog. Phys. **79**(1), 016502 (2016).
[125]J. Martinez-Vega, *Dielectric Materials for Electrical Engineering* (John Wiley & Sons, 2010).
[126]P. Morshuis, F. Kreuger, and P. Leufkens, IEEE Trans. Electr. Insul. **23**(6), 1051–1055 (1988).
[127]G. Teyssedre and C. Laurent, IEEE Trans. Dielectr. Electr. Insul. **12**(5), 857–875 (2005).
[128]Y. Sun, S. Ma, and S. A. Boggs, IEEE Trans. Dielectr. Electr. Insul. **22**(3), 1719–1722 (2015).
[129]Y. Sun, C. Bealing, S. Boggs, and R. Ramprasad, IEEE Electr. Insul. Mag. **29**(2), 8–15 (2013).
[130]Y. Sun, S. Boggs, and R. Ramprasad, Appl. Phys. Lett. **101**(13), 132906 (2012).
[131]R. Hoffmann, C. Janiak, and C. Kollmar, Macromolecules **24**(13), 3725–3746 (1991).
[132]N. K. Hindley, J. Non-Cryst. Solids **5**(1), 31–40 (1970).
[133]P. J. Walsh, J. Hall, R. Nicolaides, S. Defeo, P. Calella, J. Kuchmas, and W. Doremus, J. Non-Cryst. Solids **2**, 107–124 (1970).
[134]G. Juška and K. Arlauskas, Phys. Status Solidi A **59**(1), 389–393 (1980).
[135]K. Tsuji, Y. Takasaki, T. Hirai, and K. Taketoshi, J. Non-Cryst. Solids **114**, 94–96 (1989).
[136]K. Jandieri, O. Rubel, S. Baranovskii, A. Reznik, J. Rowlands, and S. Kasap, J. Mater. Sci.: Mater. Electron. **20**(1), 221–225 (2009).
[137]E. Voronkov, A. Popov, I. Savinov, and A. Fairushin, J. Non-Cryst. Solids **352**(9), 1578–1581 (2006).
[138]B. Ridley, J. Phys. C: Solid State Phys. **16**(17), 3373 (1983).
[139]O. Rubel, S. Baranovskii, I. Zvyagin, P. Thomas, and S. Kasap, Phys. Status Solidi C **1**(5), 1186–1193 (2004).
[140]O. Rubel, A. Potvin, and D. Laughton, J. Phys.: Condens. Matter **23**(5), 055802 (2011).
[141]L. Landau and S. Pekar, J. Exp. Theor. Phys. **18**(5), 419–423 (1948), see http://archive.ujp.bitp.kiev.ua/files/journals/53/si/53SI15p.pdf.
[142]G. De Filippis, V. Cataudella, A. Mishchenko, and N. Nagaosa, Phys. Rev. B **85**(9), 094302 (2012).
[143]J.-J. Zhou and M. Bernardi, Phys. Rev. B **94**(20), 201201 (2016).
[144]C. Verdi and F. Giustino, Phys. Rev. Lett. **115**(17), 176401 (2015).
[145]J. Sjakste, N. Vast, M. Calandra, and F. Mauri, Phys. Rev. B **92**(5), 054307 (2015).
[146]Z. Zhu, A. Chutia, H. Tsuboi, M. Koyama, A. Endou, H. Takaba, M. Kubo, C. A. Del Carpio, P. Selvam, and A. Miyamoto, Jpn. J. Appl. Phys., Part 1 **46**(4S), 1853 (2007).
[147]S. Lombardo, Microelectron. Eng. **59**(1), 33–42 (2001).
[148]K. Prasai, P. Biswas, and D. Drabold, Semicond. Sci. Technol. **31**(7), 73002–73015 (2016).
[149]R. E. Larsen, W. J. Glover, and B. J. Schwartz, Science **329**(5987), 65–69 (2010).
[150]J. Savolainen, F. Uhlig, S. Ahmed, P. Hamm, and P. Jungwirth, Nat. Chem. **6**(8), 697–701 (2014).
[151]P. Palianov, P. Martin, F. Quéré, and S. Pommeret, J. Exp. Theor. Phys. **118**(3), 489–493 (2014).
[152]D. Nordlund, H. Ogasawara, H. Bluhm, O. Takahashi, M. Odelius, M. Nagasono, L. G. Pettersson, and A. Nilsson, Phys. Rev. Lett. **99**(21), 217406 (2007).
[153]J. Zhao, B. Li, K. Onda, M. Feng, and H. Petek, Chem. Rev. **106**(10), 4402–4427 (2006).
[154]T. W. Kee, D. H. Son, P. Kambhampati, and P. F. Barbara, J. Phys. Chem. A **105**(37), 8434–8439 (2001).
[155]L. Turi and P. J. Rossky, Chem. Rev. **112**(11), 5641–5674 (2012).
[156]W. F. Schmidt, IEEE Trans. Electr. Insul. **EI-19**, 389–418 (1984).
[157]K. R. Siefermann, Y. Liu, E. Lugovoy, O. Link, M. Faubel, U. Buck, B. Winter, and B. Abel, Nat. Chem. **2**(4), 274–279 (2010).
[158]B. Abel, U. Buck, A. Sobolewski, and W. Domcke, Phys. Chem. Chem. Phys. **14**(1), 22–34 (2012).
[159]J. R. Casey, A. Kahros, and B. J. Schwartz, J. Phys. Chem. B **117**(46), 14173–14182 (2013).
[160]J. R. Casey, B. J. Schwartz, and W. J. Glover, J. Phys. Chem. Lett. **7**(16), 3192–3198 (2016).
[161]W. J. Glover and B. J. Schwartz, J. Chem. Theory Comput. **12**(10), 5117–5131 (2016).
[162]C. Gahl, U. Bovensiepen, C. Frischkorn, and M. Wolf, Phys. Rev. Lett. **89**(10), 107402 (2002).
[163]J. Stähler, J.-C. Deinert, D. Wegkamp, S. Hagen, and, M. Wolf, J. Am. Chem. Soc. **137**(10), 3520–3524 (2015).
[164]V. De Waele, S. SORGUES, P. Pernot, J.-L. Marignier, and M. Mostafavi, Nucl. Sci. Tech. **18**(1), 10–15 (2007).
[165]Y. Muroya, M. Lin, Z. Han, Y. Kumagai, A. Sakumi, T. Ueda, and Y. Katsumura, Radiat. Phys. Chem. **77**(10-12), 1176–1182 (2008).
[166]J. F. Wishart, A. M. Funston, T. Szreder, A. R. Cook, and M. Gohdo, Faraday Discussions **154**, 353–363 (2012).
[167]T. Toigawa, M. Gohdo, K. Norizawa, T. Kondoh, K. Kan, J. Yang, and Y. Yoshida, Radiat. Phys. Chem. **123**, 73–78 (2016).
[168]D. Zhu, L. Zhang, R. E. Ruther, and R. J. Hamers, Nat. Mater. **12**(9), 836 (2013).
[169]H. Murai, J. Photochem. Photobiol. C **3**(3), 183–201 (2003).
[170]R. W. Fessenden, Appl. Magn. Reson. **45**(5), 483–503 (2014).
[171]C. E. Perles and P. L. O. Volpe, J. Chem. Phys. **133**(24), 241104 (2010).
[172]J. Suomi and S. Kulmala, *Reviews in Fluorescence 2009* (Springer, 2011), pp. 47–73.
[173]J. Šima and V. Brezová, Monatsh. Chem./Chem. Mon. **132**(12), 1493–1500 (2001).
[174]A. A. Kulkarni and J. B. Joshi, Ind. Eng. Chem. Res. **44**(16), 5873–5931 (2005).
[175]M. K. Tripathi, K. C. Sahu, and R. Govindarajan, Nat. Commun. **6**, 6268 (2015).
[176]C. E. Brennen, *Cavitation and Bubble Dynamics* (Cambridge University Press, 2013).
[177]M. Takahashi, K. Chiba, and P. Li, J. Phys. Chem. B **111**(6), 1343–1347 (2007).
[178]J. R. Seddon, D. Lohse, W. A. Ducker, and V. S. Craig, ChemPhysChem **13**(8), 2179–2187 (2012).

[179]M. Alheshibri, J. Qian, M. Jehannin, and V. S. Craig, Langmuir **32**(43), 11086–11100 (2016).
[180]Y. Sun, G. Xie, Y. Peng, W. Xia, and J. Sha, Colloids Surf. A **495**, 176–186 (2016).
[181]Y. Liu and X. Zhang, "A review of recent theoretical and computational studies on pinned surface nanobubbles," Chin. Phys. B **27**(1), 014401 (2018).
[182]S. Thorpe, A. Stubbs, A. Hall, and R. Turner, Nature **296**(5858), 636–638 (1982).
[183]J. L. Parker, P. M. Claesson, and P. Attard, J. Phys. Chem. **98**(34), 8468–8480 (1994).
[184]H. Kobayashi, S. Maeda, M. Kashiwa, and T. Fujita, International Conference on Optical Particle Characterization (OPC 2014) **9232**, 92320U (2014).
[185]D. Seo, S. R. German, T. L. Mega, and W. A. Ducker, J. Phys. Chem. C **119**(25), 14262–14266 (2015).
[186]K. Ohgaki, N. Q. Khanh, Y. Joden, A. Tsuji, and T. Nakagawa, Chem. Eng. Sci. **65**(3), 1296–1300 (2010).
[187]P. Attard, Eur. Phys. J. Spec. Top. **2013**, 1–22 (2013).
[188]P. Li, M. Takahashi, and K. Chiba, Chemosphere **77**(8), 1157–1160 (2009).
[189]D. Lohse and X. Zhang, Rev. Mod. Phys. **87**(3), 981 (2015).
[190]A. Agarwal, W. J. Ng, and Y. Liu, Chemosphere **84**(9), 1175–1180 (2011).
[191]P. Kundu, S.-Y. Liu, F.-R. Chen, and F.-G. Tseng, paper presented at IEEE 29th International Conference on Micro Electro Mechanical Systems (MEMS) (2016).
[192]T. Temesgen, T. T. Bui, M. Han, T.-I. Kim, and H. Park, Adv. Colloid Interface Sci. **246**, 40–51 (2017).
[193]Z. Guo, Y. Liu, Q. Xiao, and X. Zhang, Langmuir **32**(43), 11328–11334 (2016).
[194]J. R. Seddon, E. S. Kooij, B. Poelsema, H. J. Zandvliet, and D. Lohse, Phys. Rev. Lett. **106**(5), 056101 (2011).
[195]B. Zhao, X. Wang, S. Wang, R. Tai, L. Zhang, and J. Hu, Soft Matter **12**(14), 3303–3309 (2016).
[196]H. An, G. Liu, R. Atkin, and V. S. Craig, ACS Nano **9**(7), 7596–7607 (2015).
[197]S. O. Yurchenko, A. V. Shkirin, B. W. Ninham, A. A. Sychev, V. A. Babenko, N. V. Penkov, N. P. Kryuchkov, and N. F. Bunkin, Langmuir **32**(43), 11245–11255 (2016).
[198]J. Qiu, Z. Zou, S. Wang, X. Wang, L. Wang, Y. Dong, H. Zhao, L. Zhang, and J. Hu, ChemPhysChem **18**(10), 1345–1350 (2017).
[199]M. Zhang and J. R. Seddon, Langmuir **32**(43), 11280–11286 (2016).
[200]R. Etchepare, H. Oliveira, M. Nicknig, A. Azevedo, and J. Rubio, Miner. Eng. **112**, 19–26 (2017).
[201]M. Li, L. Tonggu, X. Zhan, T. L. Mega, and L. Wang, Langmuir **32**(43), 11111–11115 (2016).
[202]T. P. Burg, M. Godin, S. M. Knudsen, W. Shen, G. Carlson, J. S. Foster, K. Babcock, and S. R. Manalis, Nature **446**(7139), 1066–1069 (2007).
[203]N. F. Bunkin, A. V. Shkirin, N. V. Suyazov, V. A. Babenko, A. A. Sychev, N. V. Penkov, K. N. Belosludtsev, and S. V. Gudkov, J. Phys. Chem. B **120**(7), 1291–1303 (2016).
[204]S. H. Oh and J.-M. Kim, Langmuir **33**(15), 3818–3823 (2017).
[205]F. Y. Ushikubo, T. Furukawa, R. Nakagawa, M. Enari, Y. Makino, Y. Kawagoe, T. Shiina, and S. Oshita, Colloids Surf. A **361**(1), 31–37 (2010).
[206]W. Chen, C. Xi, X. Su, and Z. Long, Prz. Elektrotech. **88**(9), 290–295 (2012).
[207]N. F. Bunkin and S. I. Bakum, Quantum Electron. **36**(2), 117 (2006).
[208]S. Ikezawa, M. Wakamatsu, and T. Ueda, paper presented at Sixth International Conference on Sensing Technology (ICST) (2012).
[209]J. Yang, J. Duan, D. Fornasiero, and J. Ralston, J. Phys. Chem. B **107**(25), 6139–6147 (2003).
[210]C. U. Chan and C.-D. Ohl, Phys. Rev. Lett. **109**(17), 174501 (2012).
[211]K. Yasui, T. Tuziuti, W. Kanematsu, and K. Kato, Phys. Rev. E **91**(3), 033008 (2015).
[212]X. H. Zhang, X. D. Zhang, S. T. Lou, Z. X. Zhang, J. L. Sun, and J. Hu, Langmuir **20**(9), 3813–3815 (2004).
[213]B. M. Borkent, S. M. Dammer, H. Schönherr, G. J. Vancso, and D. Lohse, Phys. Rev. Lett. **98**(20), 204502 (2007).
[214]X. Zhang, H. Lhuissier, C. Sun, and D. Lohse, Phys. Rev. Lett. **112**(14), 144503 (2014).
[215]Y. Pan, B. Bhushan, and X. Zhao, Beilstein J. Nanotechnol. **5**, 1042 (2014).
[216]J. R. Seddon, H. J. Zandvliet, and D. Lohse, Phys. Rev. Lett. **107**(11), 116101 (2011).
[217]M. P. Brenner and D. Lohse, Phys. Rev. Lett. **101**(21), 214505 (2008).
[218]T. J. Lewis, *The Liquid State and its Electrical Properties* (Springer, 1988), pp. 431–453.
[219]A. Feng, B. J. McCoy, Z. A. Munir, and D. Cagliostro, Mater. Sci. Eng.: A **242**(1), 50–56 (1998).
[220]Y. Julliard, K. Kist, R. Badent, and A. Schwab, paper presented at Annual Report Conference on the *Electrical Insulation and Dielectric Phenomena* (2000).
[221]H. Over and A. Seitsonen, Science **297**(5589), 2003–2005 (2002).
[222]J. Panter, B. Viguier, J.-M. Cloué, M. Foucault, P. Combrade, and E. Andrieu, J. Nucl. Mater. **348**(1), 213–221 (2006).
[223]J. Evertsson, F. Bertram, F. Zhang, L. Rullik, L. Merte, M. Shipilin, M. Soldemo, S. Ahmadi, N. Vinogradov, and F. Carlà, Appl. Surf. Sci. **349**, 826–832 (2015).
[224]L. E. Sanchez-Caldera, P. Griffith, and E. Rabinowicz, J. Eng. Gas Turbines Power **110**(2), 180–184 (1988).
[225]A. Gebert, K. Buchholz, A. El-Aziz, and J. Eckert, Mater. Sci. Eng. A **316**(1), 60–65 (2001).
[226]D. Nabhan, B. Kapusta, P. Billaud, K. Colas, D. Hamon, and N. Dacheux, J. Nucl. Mater. **457**, 196–204 (2015).
[227]T. Belmonte, A. Hamdan, F. Kosior, C. Noël, and G. Henrion, J. Phys. D: Appl. Phys. **47**(22), 224016 (2014).
[228]G. A. Mesyats, Phys.-Usp. **38**(6), 567 (1995).
[229]G. Mesyats, Plasma Phys. Controlled Fusion **47**(5A), A109 (2005).
[230]G. A. Mesyats, IEEE Trans. Plasma Sci. **41**(4), 676–694 (2013).
[231]R. G. Forbes, Solid-State Electron. **45**(6), 779–808 (2001).
[232]T. Lewis, IEEE Trans. Dielectr. Electr. Insul. **10**(6), 948–955 (2003).
[233]K. Mathes and J. Atkins, paper presented at IEEE International Conference on Electrical Insulation (1978).
[234]V. Goryachev, A. Ufimtsev, and A. Khodakovskii, Tech. Phys. Lett. **23**(5), 386–387 (1997).
[235]P. Lukeš, M. Člupek, V. Babický, P. Šunka, J. Skalný, M. Štefečka, J. Novák, and Z. Málková, Czech. J. Phys. **56**, B916–B924 (2006).
[236]P. Lukes, M. Clupek, V. Babicky, I. Sisrova, and V. Janda, Plasma Sources Sci. Technol. **20**(3), 034011 (2011).
[237]F. Holzer and B. R. Locke, Plasma Chem. Plasma Process. **28**(1), 1–13 (2008).
[238]N. Parkansky, B. Alterkop, R. Boxman, S. Goldsmith, Z. Barkay, and Y. Lereah, Powder Technol. **150**(1), 36–41 (2005).
[239]H. Lee, S. H. Park, S.-C. Jung, J.-J. Yun, S.-J. Kim, and D.-H. Kim, J. Mater. Res. **28**(8), 1105–1110 (2013).
[240]P. Zilio, M. Dipalo, F. Tantussi, G. C. Messina, and F. De Angelis, Light: Sci. Appl. **6**(6), e17002 (2017).
[241]R. G. Hobbs, W. P. Putnam, A. Fallahi, Y. Yang, F. X. Kärtner, and K. K. Berggren, Nano Lett. **17**(10), 6069–6076 (2017).
[242]H. Yanagisawa, S. Schnepp, C. Hafner, M. Hengsberger, D. E. Kim, M. F. Kling, A. Landsman, L. Gallmann, and J. Osterwalder, Sci. Rep. **6**, 35877 (2016).
[243]E. T. Boulais, R. M. Lachaine, and M. Meunier, Nano Lett. **12**(9), 4763–4769 (2012).
[244]P. Ball, Nature **452**(7185), 291–292 (2008).
[245]F. Franks, in *Water A Comprehensive Treatise: Aqueous Solutions of Amphiphiles and Macromolecules*, edited by H. Hauser (Plenum Press, New York and London, 1975), Vol. 4.
[246]P. Wernet, D. Nordlund, U. Bergmann, M. Cavalleri, M. Odelius, H. Ogasawara, L.-Å. Näslund, T. Hirsch, L. Ojamäe, and P. Glatzel, Science **304**(5673), 995–999 (2004).
[247]V. Petkov, Y. Ren, and M. Suchomel, J. Phys.: Condens. Matter **24**(15), 155102 (2012).
[248]T. S. Zwier, Science **304**(5674), 1119–1120 (2004).
[249]C. J. Sahle, C. Sternemann, C. Schmidt, S. Lehtola, S. Jahn, L. Simonelli, S. Huotari, M. Hakala, T. Pylkkänen, and A. Nyrow, Proc. Natl. Acad. Sci. U.S.A. **110**(16), 6301–6306 (2013).
[250]L. Zhao, K. Ma, and Z. Yang, Int. J. Mol. Sci. **16**(4), 8454–8489 (2015).
[251]A. Møgelhøj, A. K. Kelkkanen, K. T. Wikfeldt, J. Schiøtz, J. J. Mortensen, L. G. Pettersson, B. I. Lundqvist, K. W. Jacobsen, A. Nilsson, and J. K. Nørskov, J. Phys. Chem. B **115**(48), 14149–14160 (2011).
[252]T. Morawietz, A. Singraber, C. Dellago, and J. Behler, Proc. Natl. Acad. Sci. U.S.A. **113**(30), 8368–8373 (2016).
[253]I. Benjamin, *Modern Aspects of Electrochemistry* (Springer, 2002), pp. 115–179.

[254]G. Cassone, F. Creazzo, P. V. Giaquinta, F. Saija, and A. M. Saitta, Phys. Chem. Chem. Phys. **18**(33), 23164–23173 (2016).
[255]C. López-Plascencia, M. Martínez-Negrete-Vera, and R. Garibay-Alonso, Int. J. Hydrogen Energy **42**(8), 4774–4781 (2017).
[256]R. Johnson, Water **3**, 132–145 (2012).
[257]A. Widom, J. Swain, J. Silverberg, S. Sivasubramanian, and Y. Srivastava, Phys. Rev. E **80**(1), 016301 (2009).
[258]J. Jirsák, F. Moučka, J. Škvor, and I. Nezbeda, Mol. Phys. **113**(8), 848–853 (2015).
[259]L. Piatkowski, A. D. Wexler, E. C. Fuchs, H. Schoenmaker, and H. J. Bakker, Phys. Chem. Chem. Phys. **14**(18), 6160–6164 (2012).
[260]V. Oshurko, A. Ropyanoi, A. Fedorov, M. Fedosov, and N. Shelaeva, Tech. Phys. **57**(11), 1589–1592 (2012).
[261]E. C. Fuchs, B. Bitschnau, A. D. Wexler, J. Woisetschläger, and F. T. Freund, J. Phys. Chem. B **119**(52), 15892–15900 (2015).
[262]E. C. Fuchs, M. Sammer, A. D. Wexler, P. Kuntke, and J. Woisetschläger, J. Phys. D: Appl. Phys. **49**(12), 125502 (2016).
[263]M. Sammer, A. D. Wexler, P. Kuntke, H. Wiltsche, N. Stanulewicz, E. Lankmayr, J. Woisetschläger, and E. C. Fuchs, J. Phys. D: Appl. Phys. **48**(41), 415501 (2015).
[264]E. C. Fuchs, B. Bitschnau, J. Woisetschläger, E. Maier, B. Beuneu, and J. Teixeira, J. Phys. D: Appl. Phys. **42**(6), 065502 (2009).
[265]J. Woisetschläger, K. Gatterer, and E. C. Fuchs, Exp. Fluids **48**(1), 121–131 (2010).
[266]E. C. Fuchs, A. D. Wexler, A. H. Paulitsch-Fuchs, L. L. Agostinho, D. Yntema, and J. Woisetschläger, Eur. Phys. J. Spec. Top. **223**(5), 959–977 (2014).
[267]J. A. Bittencourt, *Fundamentals of Plasma Physics* (Springer Science & Business Media, 2004).
[268]J. Boeuf, L. Yang, and L. Pitchford, J. Phys. D: Appl. Phys. **46**(1), 015201 (2013).
[269]R. Ye and W. Zheng, Appl. Phys. Lett. **93**(7), 071502 (2008).
[270]J. Furmanski, J. Y. Kim, and S.-O. Kim, IEEE Trans. Plasma Sci. **39**(11), 2338 (2011).
[271]P. Vanraes, A. Y. Nikiforov, A. Bogaerts, and C. Leys, Sci. Rep. **8**, 10919 (2018).
[272]Y. Setsuhara, Arch. Biochem. Biophys. **605**, 3–10 (2016).
[273]S. Miralai, E. Monette, R. Bartnikas, G. Czeremuszkin, M. Latreche, and M. Wertheimer, Plasmas Polym. **5**(2), 63–77 (2000).
[274]X. Li, D. Niu, P. Jia, N. Zhao, and N. Yuan, Plasma Sci. Technol. **13**(2), 213 (2011).
[275]S. Hofmann, K. van Gils, S. van der Linden, S. Iseni, and P. Bruggeman, Eur. Phys. J. D **68**(3), 56 (2014).
[276]M. D. V. S. Mussard, E. Foucher, and A. Rousseau, J. Phys. D: Appl. Phys. **48**(42), 424003 (2015).
[277]D. Riès, G. Dilecce, E. Robert, P. Ambrico, S. Dozias, and J. M. Pouvesle, J. Phys. D: Appl. Phys. **47**(27), 275401 (2014).
[278]S.-Y. Yoon, G.-H. Kim, S.-J. Kim, B. Bae, N.-K. Kim, H. Lee, N. Bae, S. Ryu, S. Yoo, and S. Kim, Phys. Plasmas **24**(1), 013513 (2017).
[279]O. Björneholm, M. H. Hansen, A. Hodgson, L.-M. Liu, D. T. Limmer, A. Michaelides, P. Pedevilla, J. Rossmeisl, H. Shen, and G. Tocci, Chem. Rev. **116**(13), 7698–7726 (2016).
[280]D. Zhukhovitskii, Colloid J. **72**(2), 188–194 (2010).
[281]D. E. Otten, P. R. Shaffer, P. L. Geissler, and R. J. Saykally, Proc. Natl. Acad. Sci. U. S. A. **109**(3), 701–705 (2012).
[282]S. Ou, Y. Hu, S. Patel, and H. Wan, J. Phys. Chem. B **117**(39), 11732–11742 (2013).
[283]J. Smith and S. W. Rick, Condens. Matter Phys. **19**(2), 23002 (2016).
[284]E. Chacón, P. Tarazona, and J. Alejandre, J. Chem. Phys. **125**(1), 014709 (2006).
[285]J. Lekner, *Theory of Reflection: Reflection and Transmission of Electromagnetic, Particle and Acoustic Waves* (Springer, 2016).
[286]Y. Wu and C. Pan, Nanoscale Microscale Thermophys. Eng. **10**(2), 157–170 (2006).
[287]R. N. Dahms, J. Manin, L. M. Pickett, and J. C. Oefelein, Proc. Combust. Inst. **34**(1), 1667–1675 (2013).
[288]Q. Yan and B. Wang, Henan Chem. Indus. **4**, 007 (2015), see http://en.cnki.com.cn/Article_en/CJFDTOTAL-HNHU201504007.htm.
[289]J. M. Douillard, J. Colloid Interface Sci. **337**(1), 307–310 (2009).
[290]D. Verreault and H. C. Allen, Chem. Phys. Lett. **586**, 1–9 (2013).
[291]S. E. Sanders, H. Vanselous, and P. B. Petersen, J. Phys.: Condens. Matter **30**(11), 113001 (2018).
[292]K. Matsuzaki, R. Kusaka, S. Nihonyanagi, S. Yamaguchi, T. Nagata, and T. Tahara, J. Am. Chem. Soc. **138**(24), 7551–7557 (2016).
[293]D. Sagar, C. D. Bain, and J. R. Verlet, J. Am. Chem. Soc. **132**(20), 6917–6919 (2010).
[294]I. W. Kuo, C. J. Mundy, B. L. Eggimann, M. J. McGrath, J. I. Siepmann, B. Chen, J. Vieceli, and D. J. Tobias, J. Phys. Chem. B **110**(8), 3738–3746 (2006).
[295]P. Bruggeman, J. Van Slycken, J. Degroote, J. Vierendeels, P. Verleysen, and C. Leys, IEEE Trans. Plasma Sci. **36**(4), 1138–1139 (2008).
[296]R. M. Namin and Z. Karimi, "Dynamics of a vertical water bridge," preprint arXiv:1309.2222 (2013).
[297]W. Luedtke, U. Landman, Y.-H. Chiu, D. Levandier, R. Dressler, S. Sok, and M. S. Gordon, J. Phys. Chem. A **112**(40), 9628–9649 (2008).
[298]R. Javanshad and A. Venter, Anal. Methods **9**(34), 4896–4907 (2017).
[299]M.-Z. Huang, S.-C. Cheng, Y.-T. Cho, and J. Shiea, Anal. Chim. Acta **702**(1), 1–15 (2011).
[300]G. A. Harris, A. S. Galhena, and F. M. Fernandez, Anal. Chem. **83**(12), 4508–4538 (2011).
[301]A. R. Venter, K. A. Douglass, J. T. Shelley, G. Hasman, Jr., and E. Honarvar, Anal. Chem. **86**(1), 233–249 (2014).
[302]D. J. Weston, Analyst **135**(4), 661–668 (2010).
[303]M. Drancourt, Clin. Microbiol. Inf. **16**(11), 1620–1625 (2010).
[304]H. Chen, Z. Ouyang, and R. G. Cooks, Angew. Chem. Int. Ed. **45**(22), 3656–3660 (2006).
[305]A. Albert, J. T. Shelley, and C. Engelhard, Anal. Bioanal. Chem. **406**(25), 6111–6127 (2014).
[306]S. Brandt, F. D. Klute, A. Schütz, and J. Franzke, Anal. Chim. Acta **951**, 16–31 (2017).
[307]C. A. Guo, F. Tang, J. Chen, X. Wang, S. Zhang, and X. Zhang, Anal. Bioanal. Chem. **407**(9), 2345–2364 (2015).
[308]X. Ding and Y. Duan, Mass Spectrom. Rev. **34**(4), 449–473 (2015).
[309]S. J. Ray, F. Andrade, G. Gamez, D. McClenathan, D. Rogers, G. Schilling, W. Wetzel, and G. M. Hieftje, J. Chromatogr. A **1050**(1), 3–34 (2004).
[310]A. Bogaerts and R. Gijbels, Plasma Sources Sci. Technol. **11**(1), 27 (2002).
[311]Z. Donkó, P. Hartmann, and K. Kutasi, Plasma Sources Sci. Technol. **15**(2), 178 (2006).
[312]Q. Wang, D. J. Economou, and V. M. Donnelly, J. Appl. Phys. **100**(2), 023301 (2006).
[313]Y. Choi, J. Kim, and Y. Hwang, Thin Solid Films **506–507**, 389–395 (2006).
[314]M. Shamim, J. Scheuer, R. P. Fetherston, and J. R. Conrad, J. Appl. Phys. **70**(9), 4756–4759 (1991).
[315]G. Magnuson and C. Carlston, Phys. Rev. **129**(6), 2403 (1963).
[316]H. Winter, Prog. Surf. Sci. **63**(7), 177–247 (2000).
[317]T. Cserfalvi and P. Mezei, Fresenius J. Anal. Chem. **355**(7-8), 813–819 (1996).
[318]A. F. Gaisin and E. E. Son, High Temp. **43**(1), 1–7 (2005).
[319]A. Kutepov, A. Zakharov, and A. Maksimov, *Vacuum-Plasma and Plasma-Solution Modification of Polymer Materials* (Nauka, Moscow, 2004) (in Russian), pp. 403–418.
[320]V. Titov, V. Rybkin, S. Smirnov, A. Kulentsan, and H.-S. Choi, High Temp. Mater. Process. **11**(4), 515–525 (2007).
[321]P. Bruggeman, J. Liu, J. Degroote, M. G. Kong, J. Vierendeels, and C. Leys, J. Phys. D: Appl. Phys. **41**(21), 215201 (2008).
[322]P. Mezei and T. Cserfalvi, J. Phys. D: Appl. Phys. **39**(12), 2534 (2006).
[323]X. Lu and M. Laroussi, J. Phys. D: Appl. Phys. **36**(6), 661 (2003).
[324]A. J. Schwartz, S. J. Ray, E. Elish, A. P. Storey, A. A. Rubinshtein, G. C.-Y. Chan, K. P. Pfeuffer, and G. M. Hieftje, Talanta **102**, 26–33 (2012).
[325]K. Baba, T. Kaneko, and R. Hatakeyama, Appl. Phys. Lett. **90**(20), 201501 (2007).
[326]D. Marx, M. E. Tuckerman, J. Hutter, and M. Parrinello, Nature **397**(6720), 601–604 (1999).
[327]A. Kornyshev, A. Kuznetsov, E. Spohr, and J. Ulstrup, J. Phys. Chem. B **107**, 3351–3366 (2003).
[328]Y. Cho, C. Kim, H.-S. Ahn, E. Cho, T.-E. Kim, and S. Han, J. Appl. Phys. **101**(8), 083710 (2007).
[329]G. McCracken, Rep. Prog. Phys. **38**(2), 241 (1975).
[330]Y-i Yamamoto, Y.-I. Suzuki, G. Tomasello, T. Horio, S. Karashima, R. Mitríc, and T. Suzuki, Phys. Rev. Lett. **112**(18), 187603 (2014).
[331]P. Rumbach, D. M. Bartels, R. M. Sankaran, and D. B. Go, J. Phys. D: Appl. Phys. **48**(42), 424001 (2015).
[332]J. Zobeley, R. Santra, and L. S. Cederbaum, J. Chem. Phys. **115**(11), 5076–5088 (2001).
[333]L. Cederbaum, J. Zobeley, and F. Tarantelli, Phys. Rev. Lett. **79**(24), 4778 (1997).

[334]M. Mucke, M. Braune, S. Barth, M. Förstel, T. Lischke, V. Ulrich, T. Arion, U. Becker, A. Bradshaw, and U. Hergenhahn, Nat. Phys. **6**(2), 143–146 (2010).
[335]P. Slavicek, N. V. Kryzhevoi, E. F. Aziz, and B. Winter, J. Phys. Chem. Lett. **7**(2), 234–243 (2016).
[336]M. Shi, D. Grosjean, J. Schou, and R. Baragiola, Nucl. Instrum. Methods Phys. Res. B **96**(3-4), 524–529 (1995).
[337]H. W. Bandel, J. Appl. Phys. **22**(7), 984–985 (1951).
[338]E. Alonso, R. Baragiola, J. Ferron, M. Jakas, and A. Oliva-Florio, Phys. Rev. B **22**(1), 80 (1980).
[339]M. Radmilović-Radjenović and B. Radjenović, Contrib. Plasma Phys. **47**(3), 165–172 (2007).
[340]P. J. Bruggeman, F. Iza, and R. Brandenburg, Plasma Sources Sci. Technol. **26**(12), 123002 (2017).
[341]A. Y. Nikiforov, High Energy Chem. **42**(3), 235–239 (2008).
[342]Y. Minagawa, N. Shirai, S. Uchida, and F. Tochikubo, Jpn. J. Appl. Phys., Part 1 **53**(1), 010210 (2014).
[343]H. F. A. Verhaart and P. C. T. van der Laan, J. Appl. Phys. **55**(9), 3286 (1984).
[344]I. Gallimberti, J. Phys. Colloq. **40**(C7), C7-193–C7-250 (1979).
[345]E. Brodskaya, A. P. Lyubartsev, and A. Laaksonen, J. Chem. Phys. **116**(18), 7879 (2002).
[346]J. Kornev, N. Yavorovsky, S. Preis, M. Khaskelberg, U. Isaev, and B. N. Chen, Ozone: Sci. Eng. **28**(4), 207–215 (2006).
[347]E. C. Fuchs, A. Cherukupally, A. H. Paulitsch-Fuchs, L. L. Agostinho, A. D. Wexler, J. Woisetschläger, and F. T. Freund, J. Phys. D: Appl. Phys. **45**(47), 475401 (2012).
[348]P. Vanraes, A. Nikiforov, M. Lessiak, and C. Leys, J. Phys.: Conf. Ser. **406**(1), 012013 (2012).
[349]P. Hoffer, K. Kolacek, V. Stelmashuk, and P. Lukes, IEEE Trans. Plasma Sci. **43**(11), 3868–3875 (2015).
[350]K. Kikuchi, A. Ioka, T. Oku, Y. Tanaka, Y. Saihara, and Z. Ogumi, J. Colloid Interface Sci. **329**(2), 306–309 (2009).
[351]K. Kikuchi, Y. Tanaka, Y. Saihara, M. Maeda, M. Kawamura, and Z. Ogumi, J. Colloid Interface Sci. **298**(2), 914–919 (2006).
[352]A. V. Postnikov, I. V. Uvarov, N. V. Penkov, and V. B. Svetovoy, Nanoscale **10**(1), 428–435 (2018).
[353]H. Jablonowski, R. Bussiahn, M. Hammer, K.-D. Weltmann, T. von Woedtke, and S. Reuter, Phys. Plasmas **22**(12), 122008 (2015).
[354]S. Liu, S. Oshita, S. Kawabata, Y. Makino, and T. Yoshimoto, Langmuir **32**(43), 11295–11302 (2016).
[355]S. Liu, S. Oshita, Y. Makino, Q. Wang, Y. Kawagoe, and T. Uchida, ACS Sustainable Chem. Eng. **4**(3), 1347–1353 (2016).
[356]K. Ebina, K. Shi, M. Hirao, J. Hashimoto, Y. Kawato, S. Kaneshiro, T. Morimoto, K. Koizumi, and H. Yoshikawa, PLoS One **8**(6), e65339 (2013).
[357]A. Lindsay, B. Byrns, W. King, A. Andhvarapou, J. Fields, D. Knappe, W. Fonteno, and S. Shannon, Plasma Chem. Plasma Process. **34**(6), 1271–1290 (2014).
[358]L. Sivachandiran and A. Khacef, RSC Adv. **7**(4), 1822–1832 (2017).
[359]M. J. Traylor, M. J. Pavlovich, S. Karim, P. Hait, Y. Sakiyama, D. S. Clark, and D. B. Graves, J. Phys. D: Appl. Phys. **44**(47), 472001 (2011).
[360]J. Julák, V. Scholtz, S. Kotúčová, and O. Janoušková, Phys. Med. **28**(3), 230–239 (2012).